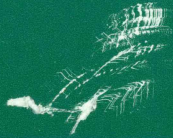U.S. Department
of Transportation

**Federal Railroad
Administration**

Task Force Report
Rail Failure Evaluation

May 1984

12 - Safety

TASK FORCE REPORT

RAIL FAILURE EVALUATION

Prepared for

the

Federal Railroad Administration

May 1984

Prepared by

U.S. Department of Transportation
Transportation Systems Center
Cambridge, Massachusetts

TABLE OF CONTENTS

EXECUTIVE SUMMARY

On November 12, 1983, an Amtrak passenger train operating on Missouri Pacific track in the vicinity of Marshall, Texas, derailed at a speed of between 70 and 75 miles per hour as it traversed a temporary track repair. The alloy rail over which the train was passing fractured and concurrently fragmented into a number of relatively small pieces. The extended length of the fracture and the concurrent fragmentation are not consistent with past experience. Similar fractures observed in standard, plain carbon steel rail generally have characteristic lengths about one third of the fracture length in the subject alloy rail, and do not exhibit fragmentation. Alloy rails of the type involved in the Marshall, Texas, derailment constitute a very small fraction of the existing domestic rail population. However, alloy rail is being used increasingly on domestic railroads because of its improved wear characteristics.

As a result of the unusual failure mode, and because of the increasing domestic usage of alloy steel to reduce rail wear, the Federal Railroad Administration requested that the Transportation Systems Center (TSC) form a Task Force to conduct a technical evaluation of the subject rail failure. The purposes of the technical evaluation were to:

o   Identify the technical factors involved in the subject rail failure.

o   Assess the safety risks, if any, associated with similar alloy rail installations.

o   Identify measures which may be used to reduce any such risks.

Based on its technical evaluation, the Task Force has found that the subject rail fracture originated at a torch-cut notch in the rail end. The fracture was a sudden, single event which was probably initiated by the impulsive overload of a lead locomotive wheel striking a rail height mismatch at high speed. The unusual extent of the fracture is believed to have resulted from adverse residual stresses existing in the subject rail.

The Task Force has concluded that exigencies requiring temporary track repairs will continue to occur in the future, and specific circumstances in some cases will result in a torch-cut rail end being left temporarily in track. Such situations are also likely to involve rail height mismatch. When a notch defect occurs in combination with a source of impulse load, the speed at which trains can safely traverse such temporary repair is limited. The maximum safe speed is theoretically lower for alloy rail than for plain carbon steel rail because certain alloy rail is less resistant to fracture than plain carbon rail steel.

The Task Force recommends that torch-cutting of rails should not be the preferred practice for temporary track repairs. However, railroads which do so to alloy rail should restrict the speed allowed over these repairs to 10 mph.

The Task Force is also of the opinion that further risks, not now present, may arise in the future as rails produced by recently introduced manufacturing procedures and/or recently developed alloy rail steels are more widely installed in domestic track. The potential for such risks is anticipated to involve combinations of routine defects, expected impulsive service loads, rail residual stress, and alloy rail products with

reduced fracture toughness. Consequently, the Task Force recommends that the industry undertake long-term studies to: (1) review all rail manufacturing processes with emphasis on quality control to insure that roller-straightening practices do not introduce adverse levels of residual stress; (2) measure the fracture toughness of various types of alloy rail steel; and (3) develop guidelines for proper alloy rail handling, installation, maintenance, and welding practices. There are no inherent reasons why acceptable combinations of manufacturing, operating, and maintenance practices cannot result in the safe use of alloy rail.

1.0 BACKGROUND

An AMTRAK passenger train (AMTRAK Train No. 21) derailed near Marshall, Texas on November 12, 1983. It has been postulated that the repair procedure used in the earlier repair of a separated rail weld was a factor in the derailment. The state of temporary repair at the time of AMTRAK train passage is shown in Figure 1.

Temporary repairs involving the removal by torch of the original chrome-vanadium alloy rail and the insertion of a temporary carbon steel plug rail with joint bars, had almost been completed, (see Figure 1c) when a west bound freight passed over the repaired section of rail at an estimated 52 mph. Following the passage of the freight train, additional temporary repairs were completed (Figure 1d), and the passenger train entered this section of the track at nearly maximum authorized speed (approximately 73 mph).
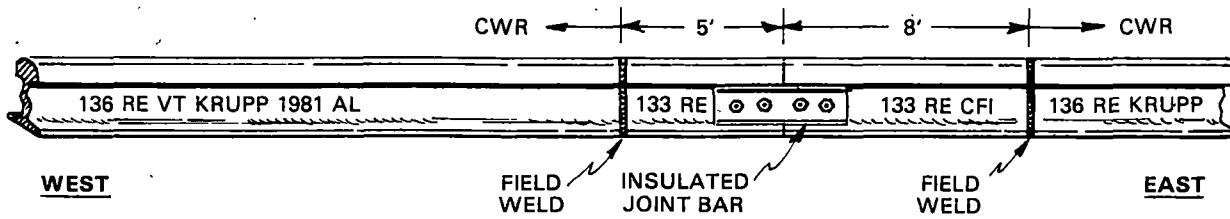
When the rail was inspected after the derailment, it was observed that at the receiving end of the chrome vanadium alloy rail (see Figure 2) there was a 93-inch longitudinal crack in the web turned up into the ball of the rail, resulting in a complete loss of this portion of the rail as indicated by battering marks on the remaining pieces of rail. An additional 25 feet of this alloy rail also failed in a seemingly unprecedented manner as the crack branched into at least 91 pieces.

Because of increasing usage of alloy steel rail as a way of reducing rail wear on domestic railroad properties, and the observed nature of the rail failure mechanism, the Federal Railroad Administration requested that the Transportation Systems Center form a Task Force to review the substantive metallurgical factors, maintenance procedures, and manufacturing processes which might be related to the observed rail failure mechanisms.
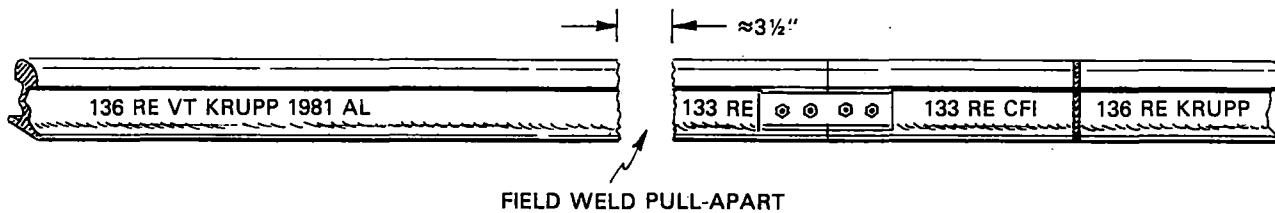
Since the events leading to the train derailment resulted from a separated rail weld between carbon and alloy steel, and possibly from procedures used during the repair of the separated weld, a brief survey was made of the rail maintenance and field-weld practices used by the domestic railroads.

The survey suggested that rail maintenance and field-weld practices were not uniform among the different rail properties. No consensus exists on special maintenance practices for alloy rail or field welding practice to be used in joining alloy rail with either alloy or plain carbon steel rail. Similarly, no consensus exists on torch cutting practices or on the slow orders to be imposed when a freight or passenger train is travelling over torch-cut rail.

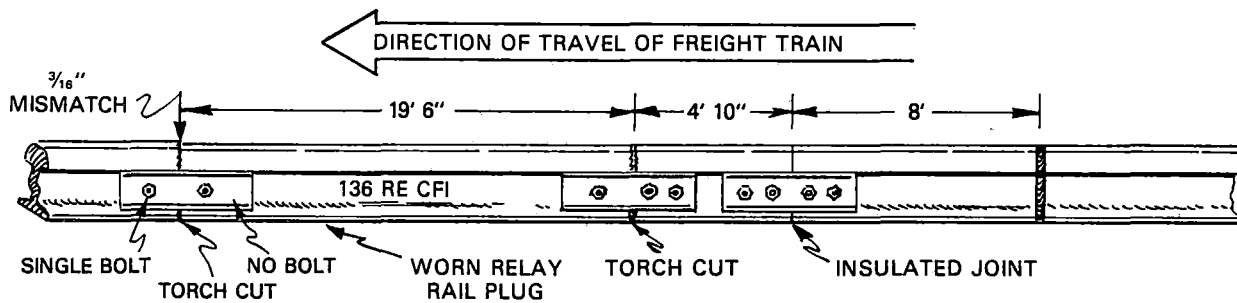The American Railway Engineering Association (AREA) was requested to provide the results of a survey on the extent of the application of alloy chrome/vanadium rails throughout the U.S. Their response (Appendix A) indicates that approximately 340 track miles (of which 300 is bolted) is in service at this time. The AREA estimated that approximately 200 miles of this track is used for AMTRAK service.

CWR ◄— ◄— 5' —► ◄— 8' —► ► CWR

| 136 RE VT KRUPP 1981 AL | 133 RE ⊙ ⊙ ⊙ ⊙ | 133 RE CFI | 136 RE KRUPP |

WEST　　　　　　　　　　　　　　　　　　　　　　　　　　　　　　**EAST**

FIELD　INSULATED　　　　FIELD
WELD　JOINT BAR　　　　WELD

1a. RAIL AS ORIGINALLY INSTALLED OCTOBER 20, 1983

◄— ≈3½" —►

| 136 RE VT KRUPP 1981 AL | 133 RE ⊙ ⊙ ⊙ ⊙ | 133 RE CFI | 136 RE KRUPP |

FIELD WELD PULL-APART

1b. RAIL PULL-PART AS DISCOVERED NOVEMBER 12, 1983 (6:49am)

◄═════ DIRECTION OF TRAVEL OF FREIGHT TRAIN ═════

3/16"
MISMATCH ↙ ◄— 19' 6" —► ◄— 4' 10" —► ◄— 8' —►

| ⊙ ⊙ | 136 RE CFI | ⊙ ⊙ ⊙ | ⊙ ⊙ ⊙ ⊙ |

SINGLE BOLT　　NO BOLT　　WORN RELAY　TORCH CUT　INSULATED JOINT
　　　TORCH CUT　　RAIL PLUG

1c. STATE OF TEMPORARY REPAIRS AT TIME OF FREIGHT TRAIN PASSAGE (9:15am)

◄═════ DIRECTION OF TRAVEL OF PASSENGER TRAIN ═════

3/16"
MISMATCH

| ⊙ ⊙ ⊙ | | ⊙ ⊙ ⊙ | ⊙ ⊙ ⊙ ⊙ |

SINGLE BOLT
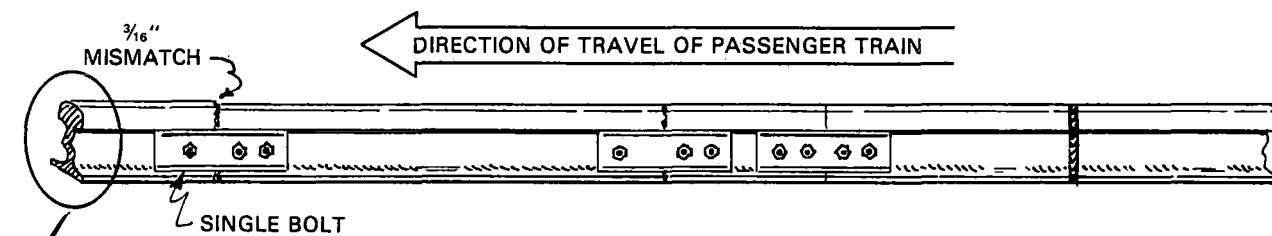
1d. STATE OF TEMPORARY REPAIRS AT TIME OF AMTRAK PASSAGE (10:10am)
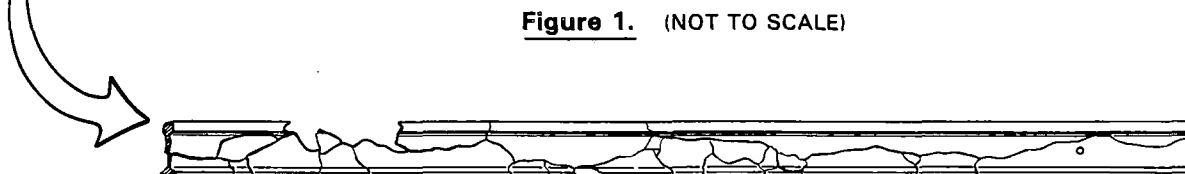
Figure 1. (NOT TO SCALE)

Figure 2. (NOT TO SCALE)

Illustration of subsequent rail break
(See detailed pullout in Appendix B)

2.0 FRACTURE ANALYSIS

Most existing installed domestic rail is made of plain carbon steel. The subject alloy rail contained significant proportions of manganese, chromium, and vanadium. Nearly all domestic observations on rail fracture have been made on plain carbon steel; the domestic railroad operating properties have only limited experience with the fracture of rails manufactured from recently introduced alloy steels. As indicated in the previous section, the alloy rail did not fracture in a manner consistent with previously observed carbon rail fractures. The purpose of the rail fracture analysis was to assess whether the observed fracture was in any way an indication that similar alloy rail installations might represent a threat to safety.

The rail fracture analysis is divided into four parts: (1) Rail Characteristics; (2) Physical and Metallurgical Examination of Rail Remnants; (3) Estimates of Rail Dynamic Loads; and (4) Discussion of Findings.

2.1 Rail Characteristics

(a) Alloy Rail Composition and Properties - Alloy rail is produced by adding various proportions of alloying elements to carbon rail steel. The principle constituents, as shown in Table 1, are silicon (Si), manganese (Mn), chromium (Cr), molybdenum (Mo), and vanadium (V). Historically, the first alloy steel rails had an increased silicon content ("Hi-Si rail") compared to that of plain carbon steel. The increased silicon content was observed to improve the rail wear characteristics. The mechanical characteristics of the different alloy steels, including the Brinell hardness number (BHN), yield strength (YS), and ultimate tensile strength (UTS) are compared in Table 1. The use of alloying elements, in general, increases rail hardness, which is associated with increased wear resistance, and increases both the yield and ultimate tensile strength. There is evidence, however, that the increased strength and improved wear resistance of rail steels which contain alloying elements in addition to the standard elements of carbon, manganese, and silicon are accompanied by reduced fracture toughness and increased fracture sensitivity. The term "alloy rail" will be used in this report to differentiate this group of rail steels from Hi-Si rail.

TABLE 1. PROPERTIES OF TYPICAL RAIL STEELS

Type	BHN	YS (ksi)	UTS (ksi)	Composition (Weight Percent)					
				C	Mn	Si	Cr	Mo	V
Plain	255	70	133	0.80	0.90	0.20	--	--	--
Hi-Si	285	75	142	0.75	0.80	0.65	--	--	--
Alloy Rail Steels:									
THS-11	326	93	157	0.70	1.00	0.70	1.00	--	0.10
1% Cr	320	94	160	0.75	0.65	0.25	1.15	--	-
Cr/Mn/V*	321	99	165	0.79	1.12	0.19	0.87	0.008	0.058
Cr/Mo	350	114	175	0.75	0.81	0.26	0.69	0.18	--

* Subject Rail

3

The limited available metallurgical data suggest that the fracture toughness of plain carbon rail steel is about 30 percent higher than the toughness of alloy rail steel which contains vanadium. (Marich, 1979). Therefore, for the same initial defect length, the critical load for alloy rail steel is about 30 percent lower than for plain carbon rail steel. (See section 2.4).

(b)   Rail Manufacture - A critical factor in the manufacture of plain carbon, Hi-Si, and alloy rail steel is the minimization of undesirable elements in the finished product. A particularly undesirable element is hydrogen which is introduced with the pig-iron charge. The presence of even small amounts of hydrogen can drastically increase the fracture sensitivity and decrease the fracture toughness of the steel rail.

In normal practice domestic rail production, after the rail has been rolled it is subject to slow controlled cooling for 24 hours which allows most of the residual hydrogen to diffuse out of the steel. Some foreign rail production practice, including that used in the production of the subject rail, utilizes a high proportion of steel scrap to decrease the initial hydrogen content. A vacuum degassing process is then applied to the molten steel to scavenge the residual hydrogen. Each rail is subsequently ultrasonically inspected to verify the absence of hydrogen flakes. These practices theoretically lead to a finished product with low hydrogen content. However, it is possible that some hydrogen flakes may go undetected, depending upon when ultrasonic inspections are performed during the manufacturing process. In such cases, the hydrogen flakes tend to form in irregular colonies, producing an irregular pattern of microcracks in the material. As a result, the rail may have a decreased fracture resistance in such regions.

Another aspect of rail manufacture of potential significance in rail fracture propagation is the method used for rail straightening. Railroad rails generally contain unwanted minor bends as they come off the rolling mill and require straightening before they are shipped. Historically, straightening practice has involved repeated applications of a concentrated load to a few discrete locations on the rail by means of a manually operated three-point bending press, ('gag-straightening'). This process has fallen out of favor because gag-straightening requires visual judgement by highly skilled operators and it is difficult to obtain uniform quality. Present practice in foreign and recently upgraded domestic rail mills, and the practice used on the subject rail, is to employ automated roller straightening. Roller straightening is, in general, more amenable to consistent quality control, but small deviations of the roller and adjustments may create large residual stresses in the rail stock. (Deroche et al., 1982). Improper gag-straightening can create similar magnitudes of residual stress. However, the residual stresses in gag-straightened rail occur at most in a few discrete locations and thus do not provide for continuous driving of a crack over an extended length during failure.

Excessive residual stresses can also be created if rails are not worked at sufficiently high temperatures in the rolling mills which form the rail cross section. In typical rail mill operations, the steel ingots from which the rail stock will be produced are held in soak pits at 2200°F until just before rolling. The rolling operation consists of three phases: working the ingot into a long billet with reduced (but still rectangular) cross section; cutting the billet into individual rails; and rolling the billets to the final length and cross section dimensions of the rail. Under normal circumstances, the entire operation takes about five minutes per ingot. Even though the material is rapidly

cooling, it remains in the upper half of the 1500-2200°F range of forging temperature during the entire operation. On occasion, however, delays in transferring ingots from the soak pit to the rolling mill or holdups between stages of the rolling operation may allow the material to cool below the nominal range for good forging and the rolling processes may create residual stresses at the lower temperatures. Such situations are usually evident during the rolling operation because the equipment tends to pound excessively as cold billets enter the rollers.

(c)   History of Alloy Rail Usage - The principal motivation for developing specialty rail steels has historically been to control the microstructure for increased hardness and better resistance to head wear. The microstructure of rail steel is formed via a crystalline phase transformation as the rail temperature drops below 1500°F after rolling.   The austenite grain structure, which is stable at higher temperatures, transforms into grains of pearlite and ferrite. Rapid cooling produces a harder, finer-grained microstructure than slow cooling.

The rate of cooling after rail rolling is limited by radiative and convective transfer of heat to the surrounding air, and is not rapid enough to produce a fine-grained microstructure.   Alloy formulations were developed, therefore, to obtain increased hardness in other ways. These formulations fall into two categories. First, Hi-Si rail steel is alloyed with extra silicon, which hardens the ferrite grains by occupying interstitial sites and thus straining the atomic lattice.   Second, additives such as chromium (Cr), columbium (Co), manganese (Mn), molybdenum (Mo), niobium (Nb), and vanadium (V) are used to slow the pearlite transformation rate. In this case, the reduced rate of pearlite transformation has the same effect as rapid cooling, i.e., a fine-grained microstructure can be produced at air-cooling rates.

The earliest attempts to produce alloy rail steels occurred over 60 years ago. Intermediate managanese (IMn) rail was manufactured and installed on the Boston & Maine Railroad in the 1920s. IMn rail manufacture actually predated the adoption of controlled cooling practice to eliminate hydrogen embrittlement. The steel used to make the IMn rail had a high sulfur content, however, and the excess sulfur apparently combined with hydrogen to alleviate the embrittlement problem. IMn rail was later found to have poor fatigue properties, and its manufacture was discontinued before this alloy saw any widespread application. Vanadium was introduced as an alloying element in an experimental rail steel in the 1920s and 1930s. Some of this early vanadium rail was installed on the Duluth, Messabi & Iron Range Railroad, but did not perform well and was never widely used.

Hi-Si rail was developed in the 1940s, and was found to have good wear and fatigue performance. It was also found that Hi-Si rail tended to give false indications of defects when tested by the magnetic induction method, although the actual incidence of defects was no worse than that of plain carbon rail. The false indication problem has declined with the advent of ultrasonic rail testing, and Hi-Si rail continues to be used today.

The early domestic alloy rail technology was pursued and further developed in Europe and Japan during the reconstruction after World War II. Some domestic suppliers responded by developing Cr-Mo rail steel alloys in the late 1960s. This was quickly followed by European and Japanese penetration of the domestic market for alloy rail and by Canadian development of Cr-Co and Cr-Nb rail in the early 1970s.

Until recently, Hi-Si and alloy rail have comprised about 5 to 10 percent of the domestic market and have been used principally on curves where plain carbon rail had experienced rapid head wear. However, wear experiments performed on the Facility for Accelerated Service Testing at the Transportation Test Center in the late 1970s have now increased the railroad industry's awareness of the wear resistance benefits obtainable with hardened rail, and the future may bring a trend of increasing usage of Hi-Si and/or alloy rail steels.

While some alloy rail steel formulations have shown improved wear resistance, the fracture toughness has generally not been considered except via the AREA specified nick-break test and drop test. These tests are measures of rail and heat homogeneity, rather than material notch sensitivity. Hence, it is possible to formulate an alloy rail steel which meets existing specifications and has improved wear resistance, but which also has reduced resistance to fracture when sharp-crack defects are present. Laboratory fracture toughness measurements have shown that domestic Cr-Mo rail steel generally has more resistance to fracture than plain carbon rail steel. However, other alloys such as chromium with high manganese or Cr-Mo with vanadium added tend to have reduced fracture resistance. Alloy rails with reduced fracture toughness are not only more sensitive to sharp-crack defects, but are also more susceptible to mechanical damage from the handling practices which have been established as reliable practices for plain carbon rails.

Other practices established on the basis of experience with plain carbon rail, such as torch-cutting and welding, can produce detrimental effects when applied to alloy rail. The process of torch-cutting actually involves flame heating of a narrow zone of the rail to oxidation temperatures, i.e., the "cut" is actually the melting and burning of the iron in the rail to produce iron oxides. An oxygen-acetylene torch provides sufficient combustion temperature to start the burning process in plain carbon rail, and the post-cut air cooling is generally slow enough to avoid the production of torch-cut defects unless an overheated flame has been used. Conversely, alloy rail requires higher temperatures to start the burning process, and is more susceptible to quench-cracking when cooling after application of an overheated flame. The tendency of alloy rail to quench-crack when torch-cut can be counteracted by following a practice of pre-heating the rail to about 930°F and making the cut with an oxygen-propane torch. However, this special practice is difficult to implement on railroad track in the field because it requires nonstandard equipment and materials and it is more time-consuming than the established practice.

Rail welding involves the heating of one or two inches of rail length to temperatures above the stable range for pearlite and ferrite, and this heat-affected zone (HAZ) retransforms to its stable microstructure as the rail cools. In the case of welding as opposed to rail-making, however, the cooling rates are much more rapid because the material outside the HAZ acts as a heat sink. Cooling of the HAZ in plain carbon rails produces an acceptable microstructure, but the transformation delay in alloy rails can lead to undesireable results. At the cooling rates which prevail in the HAZ, it is possible to reach martensite formation temperatures (about 200 to 300°F) before the delayed austenite-ferrite/pearlite reaction can occur. At these temperatures, the carbon, which is in solid solution in the austenite lattice, remains in solution as the crystal structure changes to its low-temperature form. The result is a highly strained martensite crystal structure. Martensite is an extremely hard phase, but possesses very little resistance to fracture. If the established practice for welding plain carbon

6

rail is applied to alloy rail, the HAZ may contain as much as 20 to 40 percent martensite and the weld will be susceptible to fracture under service loads. Tests of domestic CR-Mo rail have shown that increased preheating before welding is sufficient to avoid martensite in the HAZ. However, other alloy rails such as chromium with high manganese, Cr-Mn-V, and Cr-Mo-V require post-heating to maintain the HAZ above the martensite formation temperature until the austenite-ferrite/pearlite reaction can occur.

The trend toward increased usage of alloy rail is likely to continue as the long-term economic benefits are more widely recognized. Therefore, it is essential for the industry to be able to classify alloy rail steels on the basis of fracture toughness and to have specific guidelines for the manufacture, handling, installation, and maintenance of those alloys which are more notch sensitive than plain carbon rail steel.

2.2   Physical and Metallurgical Examination of Rail Remnants

(a)   Physical Examination of Rail Remnants - The subject rail remnants were examined at the Union Pacific (UP) Railroad Laboratory in Omaha, Nebraska, in December 1983. The examination included a detailed survey of the rail remnants and their fracture surfaces, and a review of the results from preliminary metallurgical tests by UP Laboratory personnel. Metallurgical tests on the subject rail fragments are continuing at the request of the Task Force and the National Transportation Safety Board. Information was also obtained from the Japanese National Railways and Wheeling Pittsburgh Steel, a rail manufacturer, about the characteristics of rail failures induced in laboratory tests of other steels. Details of the metallurgical observations summarized herein are contained in Appendix B.

A detailed fold-out diagram of the reconstructed subject rail is contained in Appendix B (Figure B-6). The fracture was about 33 feet long, and occurred primarily in the rail web. There were numerous occurrences of crack branching, in which the web crack separated into two parallel web cracks which later rejoined, or which formed separate branches which ran from the main web crack into the rail head and/or base. Virtually the entire fracture surface contained chevron markings characteristic of rapid breaking. Details of these observations appear in Appendix B, Figures B-2 through B-6.

The presence of crack branching and chevron markings implies that the fracture propagated at a speed approximating 3000 ft/sec (Bluhm, 1969). Hence, the observed rail failure is inferred to have been "sudden" in that the entire 33 feet of propagation probably required a time on the order of only 10 ms. Crack branching is not unique to the subject rail. The Japanese National Railway has observed crack branching while performing slow-bend tests on short lengths of alloy rail with different chemistry and microstructure (See Appendix B, Figure B-7). Crack branching is not ordinarily expected in a slow-bend test. For example, approximately 40 slow-bend tests were performed on plain carbon rails containing small service fatigue-crack defects as a part of the FRA/TSC rail integrity research program during 1981-1982. In all cases, these rails broke cleanly through the defect with no occurrence of crack branching. The Task Force has also arranged for additional slow-bend tests to be performed on several rails with different combinations of chemistry (alloy versus plain carbon) and roller or gag-straightening (see Table 2). In these tests, a special load fixture will be used to simulate conditions of wheel/rail vertical load and joint-bar reactions similar to the environment of the subject rail. The test rails will also be notched at the joined end to simulate the presence of a torch-cut defect.

7

TABLE 2. SAMPLES FOR SPECIAL SLOW-BEND TESTS

Type	Section	Source	Straightening	Remarks
Plain Carbon	132RE	Conrail	GAG	Service worn
Plain Carbon	132RE	Conrail	Roller	Service worn
CR/Mn/V	136RE	MoPac	Roller	New; piece of subject rail which was removed from track during temporary repair procedure
THS-11	136RE	TTC*	Roller	Service worn
1% Cr	136 RE	TTC*	Roller	Service worn
Cr/Mo	136RE	TTC*	Roller	Service worn

* Transportation Test Center

A 30-foot length is unusual for a sudden rail failure, but it lies within the order of magnitude of previous experience. Sudden failures of plain carbon steel rail have typically involved 8 to 12 feet of rail and have occurred in plain carbon steel rails that were not roller-staightened. In the case of the subject rail, residual stress is believed to have been the contributing factor that continued to drive the crack after the commencement of rapid fracture. Indirect evidence for the presence of residual stress was found in the fact that the upper and lower remnants of the subject rail were observed to be curved slightly away from each other over the first 8 feet of the fracture. The curvature indicates that the rail had been subjected to moderate plastic bending during manufacture, such as might occur in roller-straightening operations.

Any rail which had failed in stages from a series of post-derailment wheel-impact overloads could be expected to exhibit large permanent bends and several wheel marks on the gage surfaces. The absence of such bends and the paucity of wheel marks in the case of the subject rail provide additional confirmation that the failure was sudden. Figures 3 and 4 illustrate the only evidence of heavy wheel marks found anywhere on the subject rail: a web batter mark at approximately 7 feet; and a head batter mark approximately 8 feet from the torch-cut rail end. Because of their proximity these rail marks may be associated, and had to have occurred after the rail failure.

Chevron marks on a fracture surface provide a clear record of the direction of crack propagation. In the case of the subject rail, the chevron marks point unambiguously to the torch-cut rail end as the origin of the fracture. Figure 5 reveals the rail end and an inclined notch in the upper part of the web. Sectioning and scanning electron microscopy, performed by the UP, also revealed the presence of shrinkage cracking
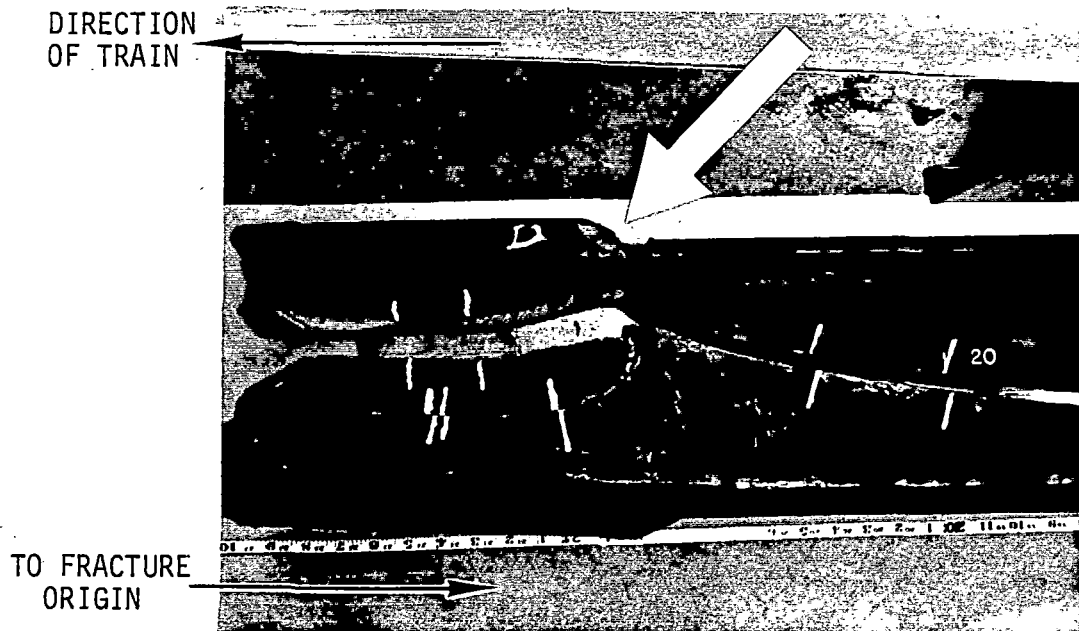
DIRECTION
OF TRAIN

TO FRACTURE
ORIGIN

FIGURE 3. WEB BATTER AT 7-FOOT MARK

DIRECTION
OF TRAIN

TO FRACTURE
ORIGIN

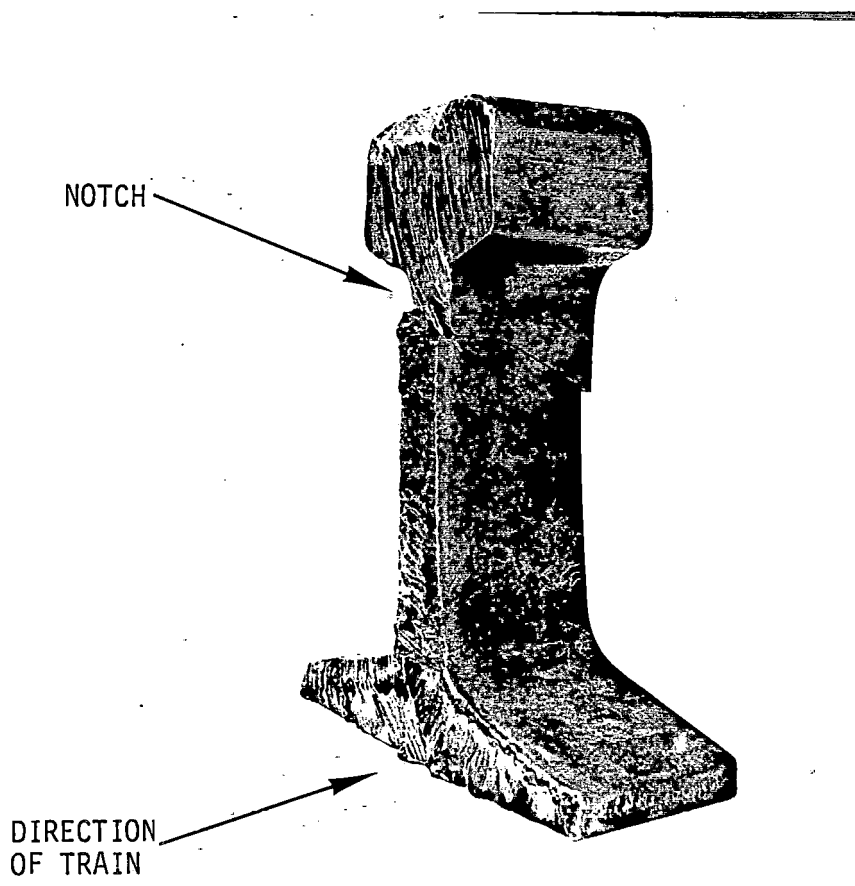FIGURE 4. HEAD BATTER AT 8-FOOT MARK

9

NOTCH

DIRECTION
OF TRAIN

FIGURE 5. PHOTO OF RAILEND

between the notch root and the beginning of the rapid fracture surface (see Figure B-1). It is, therefore, probable that the torch cutting operation left a defect in the rail end, and that this initial defect probably provided the origin for the sudden rail failure. The initial defect was in the form of a sharp-tipped crack of the order of 0.1 inch long and inclined approximately 45 degrees downward into the rail web.

The fracture features observed in the first 8 feet of the subject rail are of the type commonly associated with Mode I (opening) crack propagation. Common Mode I behavior would require a driving force acting to separate the rail head from the base, as indicated schematically in Figure 6. Such loading might be possible via reactions between the rail end and the joint bars which secured the plug rail to the subject rail. On the other hand, wheel loads might be able to drive a web crack independent of the joint-bar reactions in either of the two ways suggested in Figure 7. Details of the interaction between driving force and crack propagation can only be obtained from further tests.

(b)　Preliminary Metallurgical Examination of Rail Remnants - At the Union Pacific (UP) Railroad Laboratory, the preliminary metallurgical examinations on the subject rail did not reveal the rail to have any unusual metallurgical characteristics. The composition was close to that given by the supplier. There was no evidence of hydrogen flakes such as might have resulted from incomplete vacuum degassing. Material taken from the subject rail did, however, exhibit lower ductility than plain carbon rail steel. This lower ductility is an indicator of lower fracture toughness.

2.3　Estimate of Rail Dynamic Loads

Engineering estimates were made of the lateral, longitudinal, and vertical dynamic loads which would be expected as a function of train speed over a mismatch of the type that apparently existed at the temporary repair location. The calculations were based on a modification of a method developed by British Rail (BR) and accepted by both BR and the industry in the United States. (Jenkins et al., 1974). The original method applied to the estimation of the dynamic vertical loads at dipped rail joints. The major elements of the present modification involves replacement of the dip geometry with a step geometry corresponding to the height mismatch, and an adjustment of the wheel/rail contact stiffness to reflect corner batter at the step. Details of the model and the calculations are contained in Appendix C. The calculations show that the vertical load is larger than the lateral or longitudinal loads. The dynamic vertical load is proportional to the train speed and the square root of the mismatch height.

The vertical dynamic load resulting from the passage of the lead axle was assumed to consist of a short-time peak (P_1) and a delayed peak (P_2), as shown in Figure 8. The short-time peak is associated with battering of the rail-end corner by the upsprung mass of the lead-axle wheelset. The delayed peak is associated with rail bending (a more resilient deformation mode than corner batter). Consequently, P_1 is larger than P_2, and the difference between the short and delayed peaks increases as the train speed increases. Also, the duration (t_2) of the delayed peak is about four to ten times the duration (t_1) of the short peak. To estimate the total load at either peak, one must add the static wheel load (which depends on vehicle weight) to the dynamic load.

The total load is estimated to be approximately twice the static wheel load when the train speed is 10 mph, and the short peak can be as much as ten times the static wheel load for a 70 mph train speed. Data obtained on normal service loads as a part of the
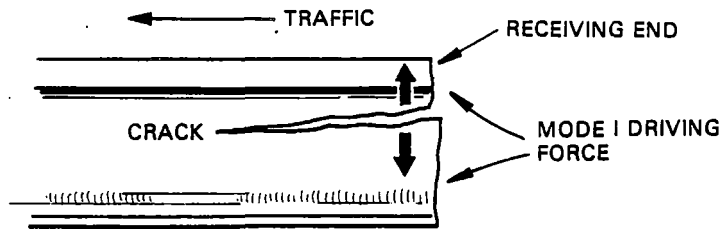
11

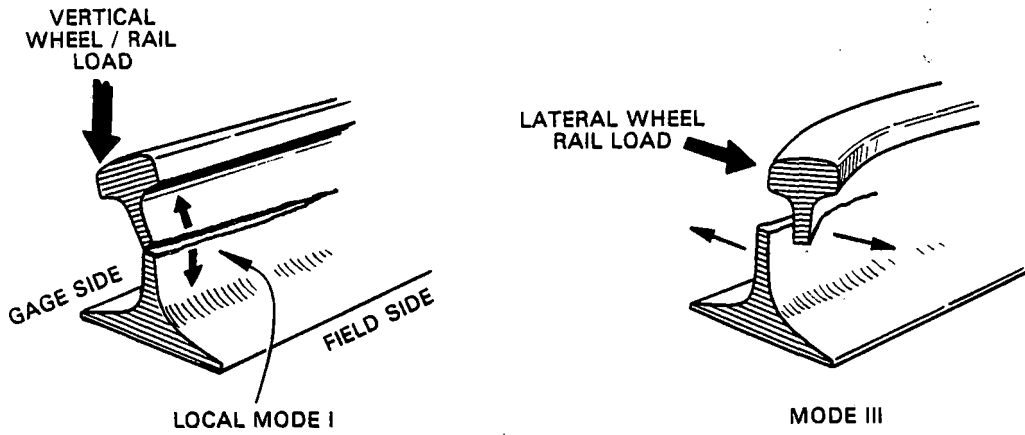FIGURE 6. COMMON MODE I LOADING OF RAIL WEB

FIGURE 7. UNCONVENTIONAL MODE I AND MODE III LOADINGS
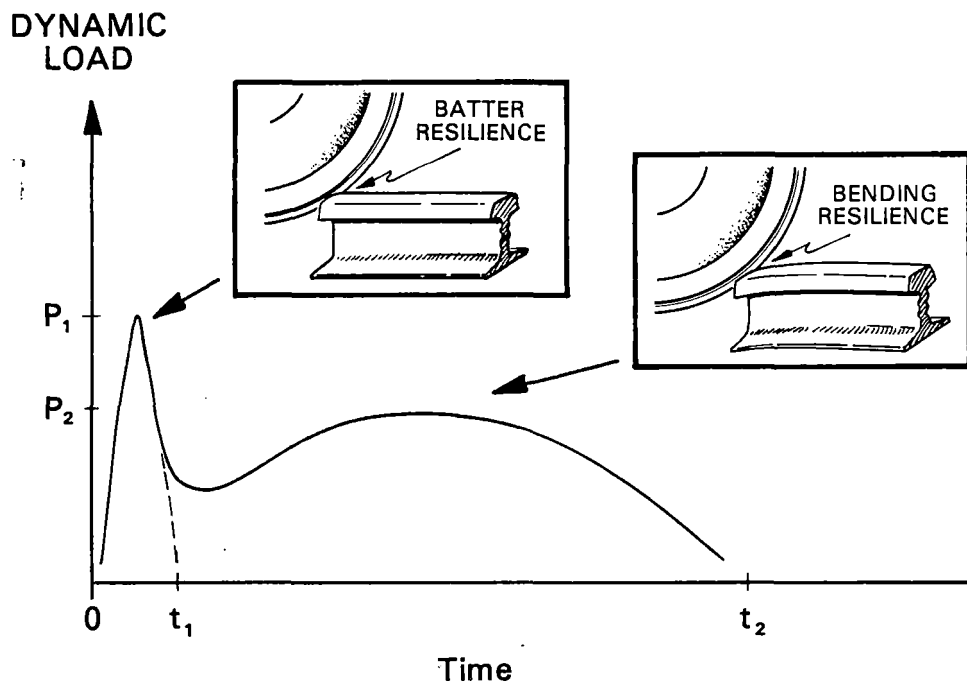EXPECTED FROM WHEEL LOAD ALONE

12

FIGURE 8. DIVISION OF DYNAMIC LOAD INTO
SHORT AND DELAYED PEAKS

13

FRA/TSC track research program shows that loads of two to three times the static wheel load occur frequently, and in rare instances wheel flats may cause loads up to six times the static wheel load in high-speed (70 mph) service. Table 3 summarizes the results of the load calculations for a locomotive axle. Peak vertical impulsive load, including the static wheel load, is shown as a function of train speed and height mismatch. Table 4 shows estimated impulse loads and duration times for both the initial and delayed peaks for a fixed height mismatch.

2.4 Discussion of Results

(a) Rail Fracture Mechanism - The observations strongly suggest that the subject rail failed suddenly, as the result of a single dynamic overload occuring when the lead wheel of the lead locomotive of the passenger train encountered a mismatch on the receiving end of the rail. Two peaks are associated with such overloads, (see discussion of Figure 8, in Section 2.3). The short-time peak is believed to be the actual cause of the failure because the short peak force is larger than the delayed force. Also, the characteristic 8 to 12 foot fracture lengths, typical of sudden failures in non-roller-straightened plain carbon steel rail correspond to propagation time of 2.5 to 4 milliseconds (ms), i.e., of the same order as the total duration of the peak dynamic loads. The propagation time estimate is based on a 3 ft/ms crack speed in steel (Bluhm, 1969).

The unusual 33-foot fracture length requires 10 ms propagation time. The additional force needed to drive this crack could have been supplied by either the delayed peak or by adverse residual stresses possibly left in the subject rail web by roller-straightening. The latter source is more likely because of the indirect evidence for the presence of residual stress, and because of the remote distance between the dynamic load application point and the extent of the fracture.

The fact that one train negotiated the repair with no apparent effect on the subject rail, while a subsequent train induced a sudden failure, bounds the critical speed range for failure of the subject rail to approximately between 50 and 70 mph. The corresponding short-peak loads can be estimated from the 50 and 70 mph rows of Table 4. Hence, the critical vertical load for failure of the rail is estimated at between 180 and 240 kips, for an assumed height mismatch of 3/16 inch.

The principles of fracture mechanics can be applied to estimate the sensitivity of plain carbon steel rail to similar loading conditions and to estimate the sensitivities of both carbon and alloy rail to operations at slower speeds. The principles of fracture mechanics lead to the following scaling law for a given alloy:

$$P\sqrt{A} = \text{Constant}$$

where A is the length of the initial crack, P is the corresponding failure load, and the constant is proportional to the alloy fracture toughness. The scaling law holds for geometrically similar situations, i.e., in the present case a 136 RE rail, with an inclined shrinkage crack at the rail end.

The available metallurgical data suggest that the fracture toughness of the subject rail is roughly half the toughness of plain carbon rail. Thus for the same initial defect length, the critical load for plain carbon rail steel should be twice the load estimated for the subject rail, i.e., between 360 and 480 kips. Applying the short-peak load

14

TABLE 3. PEAK VERTICAL IMPULSIVE LOAD AS A FUNCTION OF TRAIN SPEED AND HEIGHT MISMATCH

$$P_1 \quad = \quad P_0 + \text{Const.} \times (V) \times \sqrt{\delta}$$

Train speed	Height Mismatch (Inch)		
(mph)	1/8	3/16	3/8
10	51 kips	62 kips	88 kips
30	98	121	171
50	146	179	253
70	194	237	335

$P_0 \quad = \quad$ Static Wheel/Rail Load (33 kips)

$V \quad = \quad$ Train Velocity

$\delta \quad = \quad$ Height Mismatch

TABLE 4. INITIAL PEAK AND DELAYED PEAK AS A FUNCTION OF TRAIN SPEED AT A FIXED HEIGHT MISMATCH*

Vertical Loads

Train Speed (mph)	Initial		Delayed	
	Peak (kips)	Duration (sec.)	Peak (kips)	Duration (sec.)
10	62	0.4×10^{-3}	56	5.1×10^{-3}
30	121	0.4×10^{-3}	62	3.4×10^{-3}
50	179	0.4×10^{-3}	82	2.4×10^{-3}
70	237	0.4×10^{-3}	85	1.8×10^{-3}

* Rail Height Mismatch = 3/16 inch.

estimation procedure (Appendix C), one finds that these loads correspond to an operating speed range of approximately 110 to 150 mph. Therefore, plain carbon steel rails having defects similar to those in the subject rail would probably be subject to sudden failure only in train operations at the maximum speeds attained on any U.S. lines.

(b) Speed Restrictions - It is likely that rails will continue to be torch-cut, on occasion, when temporary track repairs are made. Railroads have long recognized the potential risks of torch cutting and have established slow orders to cover these situations. Current practices are based on the railroads' extensive experience with plain carbon rail steel.

The rail loading level is directly proportional to the train speed (see Appendix C). The speed restriction required to assure safe operation while a train is passing over a temporary repair should be slow enough to reduce considerably the size of the impulse load and the probability of rapid crack growth of a specific size rail defect.

3.0 FINDINGS, CONCLUSIONS AND RECOMMENDATIONS

FINDINGS

The Task Force has made the following findings with regard to the subject rail and its failure:

o The fracture origin was located at a notch which was left in the rail end after the rail had been torch cut.

o The fracture occurred as a sudden single event, such as would be expected to result from a single impulsive load.

o The single impulsive load which resulted in the rail fracture was probably caused by a lead locomotive wheel striking a rail height mismatch. It is estimated that the subject rail end received a vertical load of about 250,000 pounds having an impulse duration of about 2 ms.

o The estimated peak load was sufficient to initiate the rapid propagation of the rail fracture.

o The observed fracture extent can be attributed to adverse levels of residual stress believed to have been existing in the rail. Some evidence of this stress was observed during examination of the rail remnants. A manufacturing process such as roller-straightening is a possible cause of such adverse residual stress.

CONCLUSIONS

The characteristics of the subject rail failure were determined by a combination of the temporary track-repair and the properties of the rail itself. The Task Force has concluded the following with respect to both the subject rail fracture and possible similar situations:

o Temporary track repairs will continue to be used as a means of avoiding excessive train delays. In some cases, specific circumstances in the field will require the use of a torch to cut rail.

o A temporary repair which is completed by jointing a service-worn rail plug to a torch-cut rail end will leave the track in a condition which has the potential of combining a rail-end defect with a significant impulsive overload source (height mismatch).

o The foregoing conditions limit the speed at which trains can traverse such repairs without the risk of initiating rapid fracture from a rail-end defect.

o Limited experimental data indicates that the fracture toughness of alloy rail is less than that of plain carbon rail. This implies that the maximum safe speed is theoretically less for alloy rail than for plain carbon rail, given identical environments associated with temporary repairs which leave a jointed torch-cut rail end in track.

o The common practice of traversing temporary repairs at a maximum speed of 10-mph, however, reduces both impulse forces and the consequence of possible derailments to manageable levels for both alloy and plain carbon rails.

RECOMMENDATIONS

Based on the foregoing findings and conclusions, the Task Force makes the following recommendations regarding the procedures for temporary repairs which leave a torch-cut rail end jointed in track:

o The torch-cutting of rail for temporary jointed repairs should not be a preferred practice.

o If a torch-cut rail end must for any reason be left in a jointed temporary repair, railroads which do so to alloy rail should slow-order such repairs to a speed not exceeding 10 mph.

FUTURE ISSUES

The rail manufacturing technologies associated with the subject rail are within the state-of-the-art for rail manufacture. The Task Force is of the opinion that certain risks associated with these technologies may arise in the future, unless addressed by appropriate research before their widespread introduction into domestic track.

o It is likely that rail defects other than those associated with temporary repairs will continue to be inadvertently introduced into rail and track. Examples include excessively deep serial stamping, drill holes intersecting serial stamp marks, surface nicks which result from mishandling, and internal micro-crack colonies which result from excess hydrogen content. After rail has been laid, the locations of such defects can be ubiquitous and are not readily identifiable until such time as traffic loads have caused slow crack growth or rail failure.

o Impulsive overloads, such as those caused by wheel flats, can occur in track locations other than at temporary repairs. The combination of such a load with one of the foregoing defects can increase the rate of slow crack growth or cause a sudden rail failure.

o Adverse residual stress in a rail can accelerate the rate of slow crack growth or extend the length of fracture in a rail failure. Rail manufacturing processes inevitably introduce some level of residual stress in the product, but the amount is generally tolerable. However, excessive levels of residual stress may be created by process deviations such as forging a rail billet below the proper hot-working temperature or by the action of roller-straightening equipment in extending the length of highly stressed zones in a rail.

o Alloy rail development is likely to continue to result in some products with reduced ductility and fracture toughness and consequent reduced resistance to sudden failure caused by service loads. Such products may also pose relatively higher risks with respect to handling and welding.

18

In view of the foregoing points, the Task Force recommends the following long-term actions:

o   An industry study should be undertaken to assess quality control procedures to make certain that the manufacturing processes are not introducing excessive residual stresses in the product. Particular attention should be paid to the study of roller-straightening practices.

o   An industry study should be undertaken on the experimental measurement of the fracture toughness of recent formulations of alloy rail steel. Detailed information on fracture toughness and fracture susceptibility, for loading conditions characteristic of normal train operations, would provide a rational basis for the development of recommended procedures for alloy rail installation and maintenance.

o   An industry survey should be conducted to ascertain current alloy rail handling, installation, maintenance, and welding practices and produce acceptable practice guidelines since alloy rail may be less tolerant to otherwise similar practices than plain carbon rail.

4.0 BIBLIOGRAPHY

ANON, Residual Longitudinal Stresses in Rail, International Union of Railways, ORE Publication No. 25, July 1967.

Ashton, M.E., Thermit Welding of Rail Steels, Railway Engineer, Vol. 2, No. 3, 1977.

Barnsley, B.P., et al., Manufacturing Experience with a Wide Range of High Strength Rail Steels, Publication II.*

Bause, G.K., et al., Role of Alloying and Microstructure on the Strength and Toughnesses of Experimental Rail Steels, Publication I.*

Besuner, P.M., Fracture Mechanics Analysis of Rails with Shell Initiated Cracks, Publication I.*

Bhargava, P.C., Review of Latest Developments in Thermite Welding on German Railways, Indian Railway Technical Bulletin, Vol. 31, No. 193, May 1974.

Campbell, J.E., et al., Summary Report on the Examination of Rails Which Contain Detail Fractures, Proceedings American Railway Engineering Association, Vol. 51, p. 608, Appendix 10-b, June 1949.

Code, C.J., Alloy Steel Rail-Chrome-Vanadium, Penn Central Transportation Co. Test Report No. 645, January 1960.

Curcio, P., et al., Performance of High Strength Rails in Track, Publication II.*

Deroche, R.Y., et al., Stress Releasing and Straightening of Rail by Stretching, Publication IV.*

---

* Publication I refers to paper presented at ASTM Symposium on Rail Steel in Denver, Colorado, November 1976, and published in ASTM Special Technical Publication 644, Rail Steels - Developments, Processing, and Use, Stone, D.H. and Knupp, G. G., Editors, May 1978.

Publication II refers to paper presented at the Heavy Haul Railways Conference in Perth, Western Australia, September 1978 and published in the Conference Proceedings, March 1979.

Publication III refers to paper presented at Vanitec Seminar on Vanadium in Rail Steels in Chicago, Illinois, November 1979 and published in Vanitec Publication V-120, Vanadium in Rail Steels, Vanadium International Technical Committee, Westgate House, 9 Holborn, London EC1N2NE, England.

Publication IV refers to paper presented at the Second International Heavy Haul Railway Conference in Colorado Springs, Colorado, September 1982 and published in the Pre-Conference Proceedings, I.H.H.C., Inc., P.O. Box 11157, Pueblo, Colorado 81001.

Dilewijns, J., et al., Development of a Low Carbon Vanadium-Copper-Chromium Rail Steel of Improved Weldability for Curves and Points in European Railways, Publication III.*

Dohse, R., Residual Stresses in Alumino - Thermally Welded Rails, Schweissen und Schneiden, Vol. 19, No. 10, October 1967, in German.

Evans, P.R.V., et al., Fatigue Crack Growth And Sudden Fast Fracture In Rail, Journal of Iron and Steel Institute, Vol. 208, No 6, p. 560, June 1970.

Fletcher, F.B.. and Y.E. Smith, Development of High-Strength Chromium-Molybdenum Rail Steel With Improved Weldability, Publication II.*

Fletcher, F.B., et al., Fast-Welding Chromium-Molybdenum-Vanadium Extra Strength Rail Steels, Publication III.*

Fricke, H.D., Thermit Welding of Chromium-Vanadium Rail Steel, Publication III.*

Groom, J.J., Determination of Residual Stresses in Rail, Report No. FRA/ORD-83/05, May 1983.

Hauser, D., Methods for Joining of Rails: Survey Report, Report No. FRA/ORD-77/16, 1977.

Heller, W. and R. Schweitzer, Hardness, Microstructure, and Wear Behavior of Rail Steel, Publication IV.*

Heller, W., et al., Production of Special-Grade Naturally Hard Rail in Germany and Experience Gained in Operations, Publication IV.*

Heller, W. and R. Schweitzer, High Strength Pearlitic Steel Does Well in Comparative Tests of Alloy Rails, Railway Gazette International, p. 855 October 1980.

Heller, W., et al., Naturally Hard Special Grade Rail For Heavy Duty Transportation, Publication II.*

Heller, W. and R. Schweitzer, On Thermite Welding of Naturally Hard Rails of Special Cr-Mn Steels, Eisenbahn-technische Rundschau, Vol. 24, No. 10, 1975, in German.

Heller, W., Investigation of Service Behavior of Rails, Stahl und Eisen, Vol. 94, No. 4, 1974, in German.

Heller, W. and G. Schumacher, Rails for Highly Stressed Tracks, Technische Mitteilungen Krupp, Werksberichte, Vol. 32, No. 1, March 1974, in German.

Heller, W. and R. Schweitzer, Investigations Into Service Behavior of Rails, Archiv fur Eisenbahn-Technik, No. 28, 1973, in German.

Heller, W., et al., On The Effect of Hydrogen in Rail Steel and Possibilities of Hydrogen Depressing Melting Operations, Stahl und Eisen, Vol. 92, No. 19, September 1972.

BIBLIOGRAPHY (continued)

Heller, W., Manufacture, Properties, and Service Behavior of Self-Hardened Rails of Chromium-Manganese Steel With Minimum Tensile Strength of 110 kg/mm^2, Eisenbahntechnische Rundschau, Vol. 21, No. 5, 1972, in German.

Heller, W. et al., Conference On Track Construction, Stahl und Eisen, Vol. 91, No. 7, April 1971, in German.

Heller, W., On The Development And Improvement Of The Quality And Service Properties of Present Day Rail Steels, Eisenbahntechnische Rundschau Vol. 20, No. 1, 1971, in German.

Heller, W., Rail Production In Great Britain, United States, Canada, and Japan, Stahl und Eisen, Vol. 90, No. 17, August 1970, in German.

Heller, W. and G. Beck, Transformation Characteristics of Rail Steels And Their Effects On Welding And Flame Cutting, Archiv fur Eisenhuttenweisen, Vol. 39, No. 5, May 1968, in German.

Heller, W. and W. Simon, Investigation Of Joints In Continuous Rails Produced By The Secheron Welding Process, Schweizer Archiv, Vol. 33, No. 8, August 1967, in German.

Heller, W. and W. Janiche, Mechanical Properties Of Rail Steels As Affected By Flash Butt And Thermite Welding; Archiv fur Eisenhuttenwesen, Vol. 36, No. 5, May 1965, in German.

Heller, W. and W. Janiche, Change In Mechanical Properties Of Rail Steel By Hydrogen Effusion, Stahl und Eisen, Vol. 83, No. 3, January 1963, in German.

Hodgson, W. H., et al., Development of Second Generation of Alloy Steel Rails for Heavy Haul Applications, Publication IV.*

Ichinose, H., et al., An Investigation on Contact Fatigue and Wear Resistance Behavior in Rail Steels, Publication II.*

Ichinose, H., et al., High-Strength Rails Produced by Two-Stage Heating and Slack Quenching, Publication IV.*

Ito, A., New Rail Steels for Head-Hardened Crossings of Welded Construction. Railway Technical Research Institute, JNR, Quarterly Reports, Vol. 14, No. 1, March 1973.

Jenkins, H. H., et al., The Effect of Track and Vehicle Parameters on Wheel/Rail Vertical Dynamic Force, Railway Engineering Journal, Vol. 3, No. 1, January 1974.

Johns, T.G., et al., Engineering Analysis of Stresses in Railroad Rails, Report No. FRA/ORD-81/51, 1981.

Lugg, P.J., British Rail Experience With Rail Welding, Publication IV.*

BIBLIOGRAPHY (continued)

Marich, S. and P. Curcio, Development of High-Strength Alloyed Rail Steels Suitable for Heavy Duty Applications, Publication I.*

Marich, S., Flash Butt Welding of Heavy Duty Rails - Laboratory Simulation and On-Site Experience, Metals Technology Conference, Australian Institute of Metals, Melbourne, 1976.

Marich, S., et al., Laboratory Investigation of Transverse Defects in Rails, Publication II.*

Marich, S., Development of Improved Rail and Wheel Materials, Publication III.*

Masubuchi, K. and V. J. Papazoglou, Assessment of Potential for Field Welding as Method for Repairing Rail Fatigue Defects - Report to Transportation Systems Center, Cambridge, MA, June 1981.

Masumoto, H., et al., Some Features and Metallurgical Considerations of Surface Defects in Rail Due to Contact Fatigue, Publication I.*

Masumoto, H., et al., H. Development of Wear Resistant and Anti-Shelling High Strength Rails in Japan, Publication II.*

Murray, G.B., Differing Welding Techniques Aid Laying of South Africa Railway Line, Welding and Metal Fabrication, Vol, 47, No. 9, November 1979.

Mutton, P., Rail Assessment, Publication IV.*

Myers, J., Evaluation of Thermite - Type Railroad Welds, Masters Thesis, Department of Metallurgical Engineering, University of Arizona, April 1979.

Myers, J., et al., Structure and Properties of Thermite Rail Welds, Welding Journal Welding Research Supplement, August 1982.

Oliveira, J.H.S., Special Rails on Heavy Haul Railways, Publication II.*

O'Rourke, M.D., et al., Towards the Design of Rail Track for Heavy Axle Loads, Publication II.*

Park, Y.J. and I. M. Bernstein, Mechanism of Cleavage Fracture in Fully Pearlitic 1080 Rail Steel, Publication I.*

Park, Y.J. and F. B. Fletcher, Fatigue Behavior and Fracture Toughness of Standard Carbon and High Strength Rail, Publication IV.*

Ravitskaya, T.M., Features of Initiation and Development of Internal Fatigue Cracks, Strength of Materials, Vol. 6, p. 1374, 1974.

Reinders, F. and W. Heller, Production of Rail Steels of Low Hydrogen Content According To The Basic Oxygen Converter Process, Stahl und Eisen, Vol. 90 , No. 26, p. 1489, December 1970, in German.

24

BIBLIOGRAPHY (continued)

Sage, A.M., et al., The Manufacture and Railroad Trials with Chromium-Vanadium Steel for Heavy Duty Service, Publication III.*

Schilling, C.G. and G. T. Blake, Measurement of Triaxial Residual Stresses in Railroad Rails, AAR Technical Report R-447, Rail Analysis Vol. 10, March 1981.

Schmedders, H., et al., Chromium-Vanadium Rail Steel for Maximum Service Loads, Thyssen Tech. Ber., 1979, Vol. 11, pp. 60-69, in German.

Schmedders, H., A Chromium-Vanadium Alloyed Steel for Heavy Duty Requirements, Publication III.*

Schroeder, L.C. and D. R. Poirier, Mechanical Properties of Thermite Welds in Premium Alloy Rails, Material Science and Engineering, Vol. 63, p. 1, January 1984.

Schumacher, W. and W. Heller, Wear-Resistant Rail Performs Well On The Gotthard, Railway Gazette International, Vol. 129, No. 3, p. 298, August 1973.

Smith, Y.E., and F. B. Fletcher, Alloy Steels for High-Strength, As-Rolled Rails, Publication I.*

Stephenson, E.T., et al., Strengthening Mechanisms in Mn-V and MN-V-N Steels, ASME, Transactions, Vol. 57, 1964.

Sugino, K. et al., Development of Weldable High Strength Rails, Publication IV.*

Suresh, S., Crack Deflection: Implications for Growth of Long and Short Fatigue Cracks, Metallurgical Transactions, Vol. 14A, p. 2375, November 1983.

Swindale, J.D., Rail Steels: Meeting Report, Journal of the Iron and Steel Institute, Vol. 211, No. 5, p. 326, May 1973.

Timoshenko, S. and B. F. Langer, "Stresses in Railroad Track", ASME Transactions, Vol. 54, 1932.

Vines, M.J., et al., The Flash Butt Welding of High Strength Rail, Publication II.*

Wise, S., Why Metals Break, Journal of the Institute of Mechanical Engineers, Railway Division, Vol. 2, Part 2, p. 162, February 1971.

Young, J.D. and W. H. Hodgson, The Development and Manufacture of High Tensile Wear Resistant 1% Chromium Rails for Heavy Duty Applications, Publication II.*

BIBLIOGRAPHY OF AREA BULLETINS

Causes of Shelly Spots and Head Checks in Rail-Report on Assignments, Service Tests on Burlington Railroad Fort Morgan CO, of Joint Bars of Different Metallurgies, by L.S. Crane, et al., ibid., Vol. 54, p. 1237, February 1953.

Causes of Shelly Spots and Head Checks in Rail: Methods for Their Prevention -Report on Assignment 8, by L.S. Crane, et al., ibid., Vol. 55, p. 828, March 1954.

Causes of Shelly Spots and Head Checks in Rail: Methods for Their Prevention -Report on Assignment 8, by L.S. Crane, et al., ibid., Vol. 57, p. 830, September 1955.

Eighth Progress Report of Shelly Rail Studies at University of Illinois, Appendix 10a, by R.E. Cramer, ibid., Vol. 51, p. 598, June 1949.

Evaluation of Cr-Cb Alloy Rail Produced by the Sydney Steel Corporation, J.W. Cruise, et al., ibid., Vol. 78, p. 440, January-February 1977.

Evolution of Rail Steel and Rail Sections and What is Being Done Relative to This Material Today by K.W. Schoenberg, ibid., Vol. 76, p. 653, June-July 1975.

Fifteenth Progress Report of Rolling-Load Tests of Joint Bars, by R.S. Jensen, et al., ibid., Vol. 58, p. 1005, June 1956.

High-Strength Cr-Mo Rails, ibid., p. 621, June-July 1976. Y.E. Smith, et al.,

Investigation of Failure in Control-Cooled Railroad Rail, by R.E. Cramer, ibid., Vol. 58, p. 965, June 1956.

Ninth Progress Report of Shelly Rail Studies at University of Illinois, Appendix 10a, by R.E. Cramer, ibid., Vol. 52, p. 664, June 1950.

Progress Report of Rolling-Load Tests on Engine-Burned Rails, Report on Assignment 11, by F.S. Hewes, et al., Proceedings American Railway Engineering Association, Vol. 49, p. 435, June 1947.

Rail Research and Development, Part 2: Summary of Heat-Treated and Alloy Rail Service Test Installations on Curves with Shelly Histories - 1972, by W.J. Cruse, et al., ibid., Vol. 75, p. 39, September-October 1973.

Rail Steel Chemistry Review - Laboratory and Field Service Tests of Alloy and Heat-Treated Rail, by W.J. Cruse, et al., ibid., Vol. 74, p. 328, January-February 1973.

Report on Inspections of Service Tests of Heat Treated and Alloy Rail in Shelly Territory Installations, Anon., ibid., Vol. 59, p. 954, June 1957.

Report on 1962 Inspections of Service Tests of Heat-Treated and Alloy Steel Rail, by K. Kannowski, ibid., Vol. 64, p. 530, January 1963.

BIBLIOGRAPHY OF AREA Bulletins (continued)

Report on Service Tests of Heat-Treated and Alloy Rail, by K. Kannowski, ibid., Vol. 60, p. 919, March 1959.

Research on Rail Metallurgy, S. Marich, ibid., Vol. 78, p. 594, June-July 1977.

Service Tests of Heat-Treated and Alloy Steel Rail, Anon., ibid., Vol. 62, January 1961.

Service Tests of Heat-Treated and Alloy Steel Rail, Anon., ibid., Vol. 63, p. 533, February 1962.

Summary of 1969 Inspection of Heat-Treated and Alloy Rail Service Test Installations on Curves with Shelly Histories, C.F. Parvin, et al., ibid., Vol. 71, p. 688, February 1970.

Summary of Performance of Standard Carbon and Various Wear-Resistant Rails in Test Curves on the Chessie System - Second Report, by K.W. Schoenberg, ibid., Vol. 77, p. 55, September-October 1975.

Summary of Rolling-Load Tests in Cradle Machine, Appendix 11a, by R.E. Cramer, ibid., Vol. 50, p. 538, June 1948.

Tenth Progress Report of Shelly Rail Studies at University of Illinois, by R.E. Cramer, ibid., Vol. 53, p. 902, June 1951.

Test Installation of High-Silicon, High Silicon-Vanadium and High-Silicon-Vanadium-Chromium Steel Rails, by J.R. Zadra, ibid., Vol. 65, p. 534, February 1964.

Thirteenth Progress Report on Shelly Rail Studies at the University of Illinois, by R.E. Cramer, ibid., Vol. 56, p. 954, September 1954.

APPENDIX A

AREA SURVEY OF ALLOY RAIL POPULATION

**AMERICAN RAILWAY
ENGINEERING ASSOCIATION**

*2000 L St., N.W.
Washington, D.C.
20036
(202) 835-9336*

February 6, 1984

Mr. H. D. Reed
Chief, Railway Safety Division
U.S. Department of Transportation
Transportation Systems Center
Kendall Square
Cambridge, MA 02142

Dear Mr. Reed:

In response to your verbal request, we have made a survey of railroads represented on the AAR Engineering Division General Committee as to the amount of chrome vanadium alloy rail that was laid after 1972 that is presently in track. The responses included all U.S. railroads of gross revenues of over 400 million per year.

The total track miles of chrome vanadium alloy rail indicated in the replies was 340, of which at least 300 miles was bolted rail not continuously welded. An additional 36 track miles of this type of rail is installed on Canadian roads.

In regard to your question as to what percentage of this is in passenger service, Amtrak indicated that it has no chrome vanadium alloy rail on trackage that it owns or maintains. An educated guess would be that Amtrak trains presently use about 200 miles of the trackage with chrome vanadium alloy rail.

Sincerely,

Louis T. Cerny
Executive Director

LTC/met

cc: A. W. Johnston

A-3

APPENDIX B

METALLURGICAL OBSERVATIONS

APPENDIX B

DETAILS OF METALLURGICAL OBSERVATIONS

Members of the Task Force examined the failed rail at the Union Pacific Railroad Laboratory in Omaha, Nebraska on December 12, 1983. The examiners made the following observations:

1. The alloy composition, as measured by UP, is close to the nominal composition given by the rail supplier.

2. The composition of 0.87Cr, 1.12Mn, and 0.058V (plus other elements) amounts to a high-chrome/high-manganese rail rather than a nominally designated chrome-vanadium rail. The latter type of alloy usually contains 0.10V to 0.15V.

3. The torch cut on the receiving end of the rail contained a notch, with a 1/16 to 1/8 inch offset. The nick was located in the fillet region just below the rail head. See Figure 5 in Section 2.2.

4. SEM photographs of the notch showed obvious dendritic microstructure, and shrinkage cracks. (Figure B-1). The shrinkage cracks connected to the principal web crack that was involved in the rail failure.

5. The web crack ran for approximately thirty feet, undulating up and down in the web. The crack orientation was straight through for about the first two-thirds of the distance, and at 45 degrees to the horizontal for the last third. The following additional features were observed, with the approximate distances from the receiving end of the rail noted.

6   Featureless granular fracture surface (first 4 to 5 inches), Figure B-2.

7. Chevron markings appeared, symmetrical across web thickness, with bottom of V pointing back toward the receiving end (5 inches), Figure B-2. Similar chevron markings were ubiquitous thereafter.

8. Web crack ran up toward head, passing over the drilled bolt hole. A water mark appears on fracture surface (12 to 18 inches).

9. Three rubbing marks on lower surface (web/base piece) of web crack, but no corresponding marks on upper surface (2 to 6 feet).

10. Crack branching in web and into base, with chevrons indicating propagation both away from and then reversing toward receiving end of rail on different branches at 6 to 7 feet, Figure B-3.

11. Heavy batter and blue discoloration on an inclined branch (going up and away from receiving end) of the web crack: A damaged area can be seen near the top of the incline, where branch rejoins main web crack underneath rail head at 7 feet. See Figure 3 in Section 2.2.

12. First branch breaking out to rail head and receiving end of broken rail head heavily battered at 8 feet. See Figure 4 in Section 2.2.

B-3

DIRECTION
OF TRAIN

1MM   30KU   11   020   S
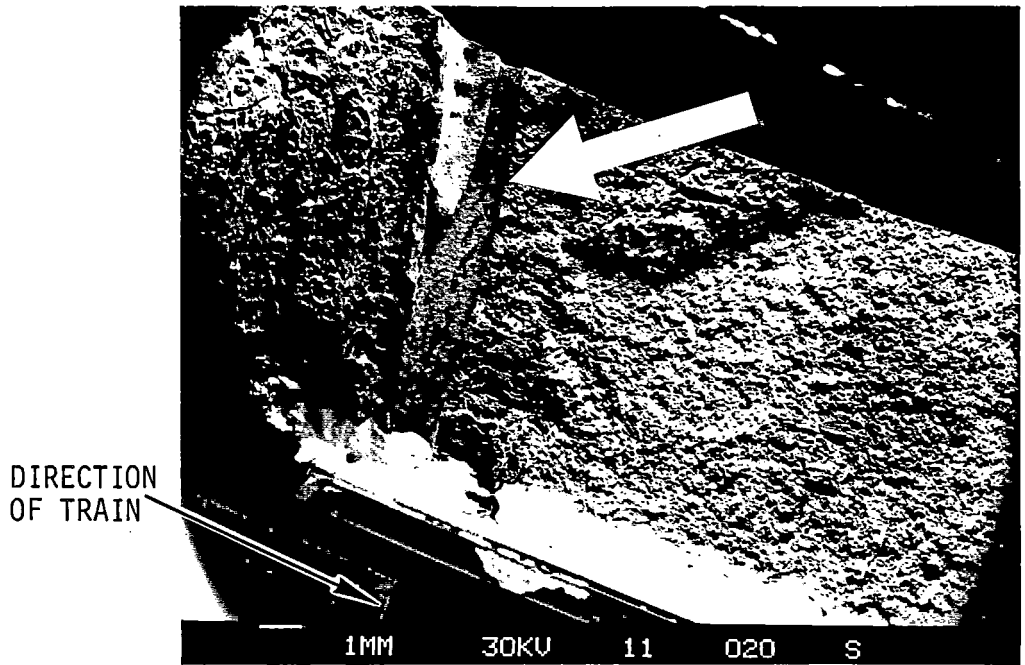
FIGURE B-1. SEM PHOTO OF FRACTURE SURFACE AT ORIGIN
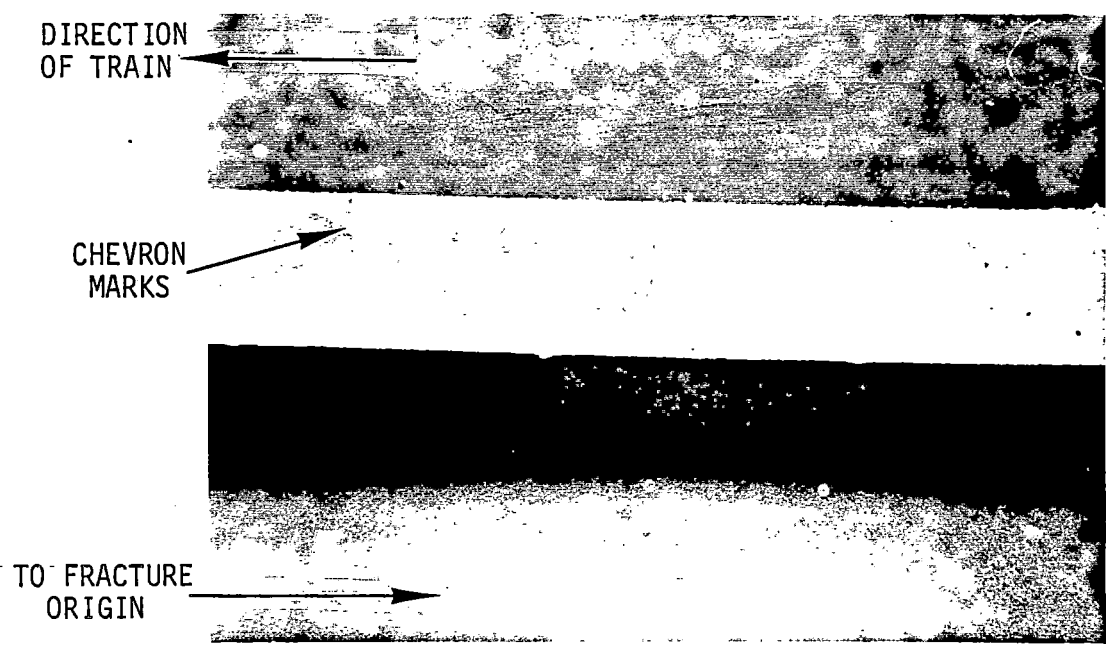
DIRECTION
OF TRAIN

CHEVRON
MARKS

TO FRACTURE
ORIGIN

FIGURE B-2.   VIEW LOOKING DOWN AT FIRST 4 TO 5 INCHES
OF RAIL WEB FRACTURE

B-4

DIRECTION OF TRAIN

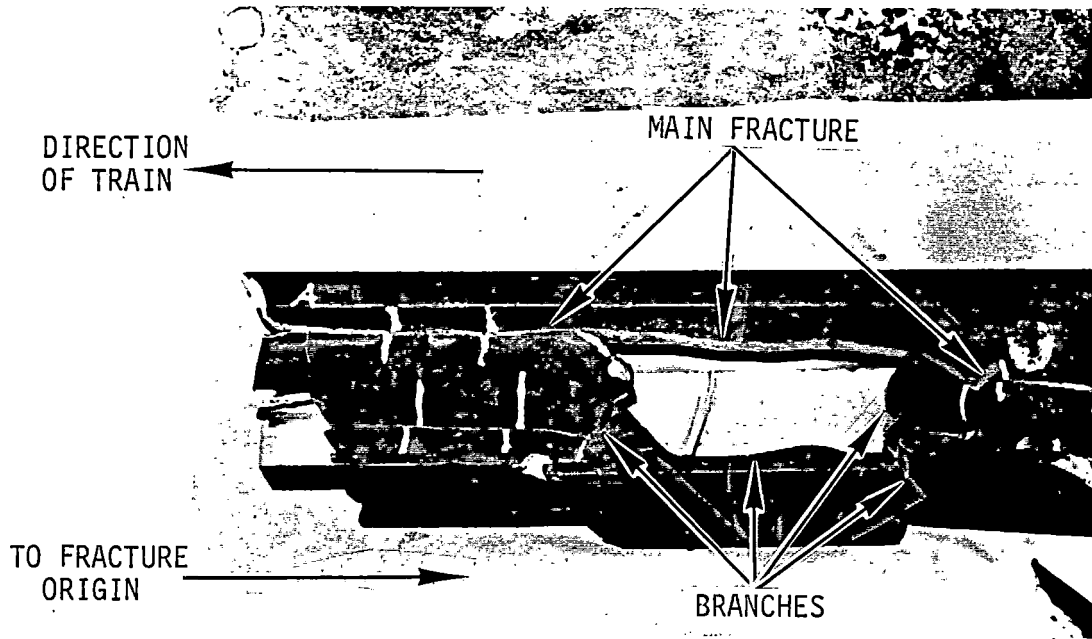MAIN FRACTURE

TO FRACTURE ORIGIN

BRANCHES

FIGURE B-3. EXAMPLE OF CRACK BRANCHING

13. Crack branching similar to Item (10), with one case of branching including breakout to rail head (10 to 21 feet). Minor batter was observed on receiving end of head breakout (21 feet).

14. Web crack ran through plant weld (19 feet).

15. Shattered zone approximately 1 to 2 feet long, with pieces of the order of 1 to 2 inches long at 20 feet, Figure B-4.

16. After the shattered zone, web crack orientation changed to 45 degrees for the remaining length of the failure; highly fluted chevron markings appear on this part of the crack, Figure B-5.

17. There were no observations of any beachmarks indicating crack arrest.

18. Visual observation did not reveal any evidence of hydrogen cracking.

19. No large-scale plastic bending was observed. The first 8 feet of the web crack did exhibit apparent elastic stress relief, however, as indicated by the fact that the fracture surfaces could not be mated along the entire length without a gap.

A detailed illustration of the failed rail is reproduced here in Figure B-6 to locate the foregoing observations. Figure B-6 also records the directions of crack propagation inferred from chevron markings.

Related information was obtained from the Japanese National Railway (JNR) on fracture tests of alloy rail with similar chrome and manganese content and comparable strength to that of the failed rail. Two short lengths of the JNR rail were broken in the laboratory by means of a three-point bending test. Although the load was applied slowly these rails broke in a crack-branching pattern similar to the observations noted in Items 10. and 13. above (Figure B-7). Table B-1 compares the alloy composition, showing that the JNR and failed rails have similar contents of chromium (Cr), manganese (Mn), and vanadium (V), but the carbon content of the JNR rail is much lower than that of plain carbon or conventional alloy rail steels.

TABLE B-1. COMPOSITIONS REPORTED FOR ALLOY RAILS (Wt%)

Element	CR	Mn	V	C	Si	Mo	Ni	S	P	B	Al
Failed Rail	0.87	1.12	0.058	0.79	0.19	0.008	0.037	0.025	0.015	---	---
JNR L22063	1.15	1.18	0.07	0.33	0.32	0.20	---	0.007	0.020	0.0022	0.024
JNR L22061	1.14	1.22	0.06	0.33	0.29	0.19	---	0.007	0.019	0.002	0.019

DIRECTION
OF TRAIN

TO FRACTURE
ORIGIN

FIGURE B-4. SHATTERED ZONE

TO FRACTURE
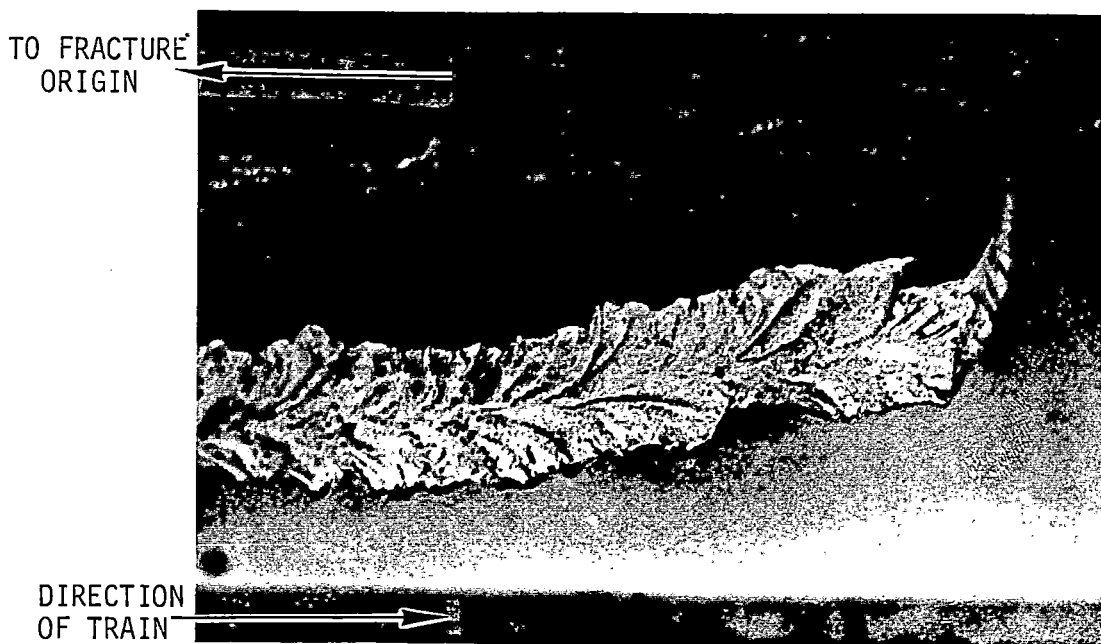ORIGIN

DIRECTION
OF TRAIN
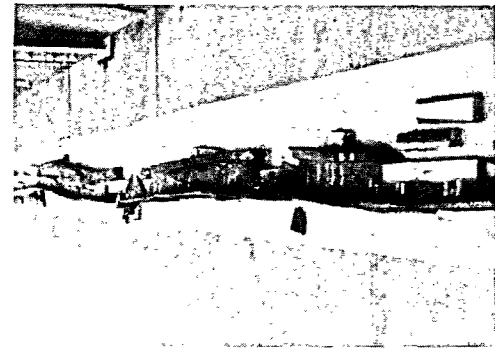
FIGURE B-5. PHOTO OF INCLINED FRACTURE SURFACE

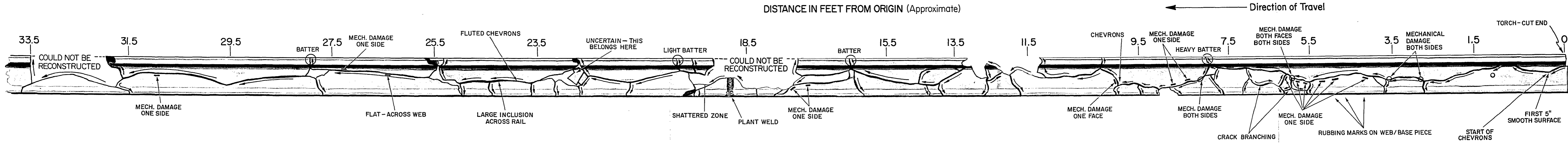Photograph of Reconstruction in UPRR Laboratory, looking from 9.5 foot mark toward 33.5 foot mark

DISTANCE IN FEET FROM ORIGIN (Approximate)

← Direction of Travel

33.5 31.5 29.5 27.5 25.5 23.5 18.5 15.5 13.5 11.5 9.5 7.5 5.5 3.5 1.5 0

BATTER

MECH. DAMAGE ONE SIDE

FLUTED CHEVRONS

UNCERTAIN – THIS BELONGS HERE

LIGHT BATTER

BATTER

CHEVRONS

MECH. DAMAGE ONE SIDE

HEAVY BATTER

MECH. DAMAGE BOTH FACES BOTH SIDES

MECH. DAMAGE BOTH SIDES

MECHANICAL DAMAGE BOTH SIDES

TORCH–CUT END

COULD NOT BE RECONSTRUCTED

COULD NOT BE RECONSTRUCTED

MECH. DAMAGE ONE SIDE

FLAT–ACROSS WEB

LARGE INCLUSION ACROSS RAIL

SHATTERED ZONE

PLANT WELD

MECH. DAMAGE ONE SIDE

MECH. DAMAGE ONE FACE

MECH. DAMAGE BOTH SIDES

MECH. DAMAGE ONE SIDE

CRACK BRANCHING

RUBBING MARKS ON WEB/BASE PIECE

START OF CHEVRONS

FIRST 5" SMOOTH SURFACE

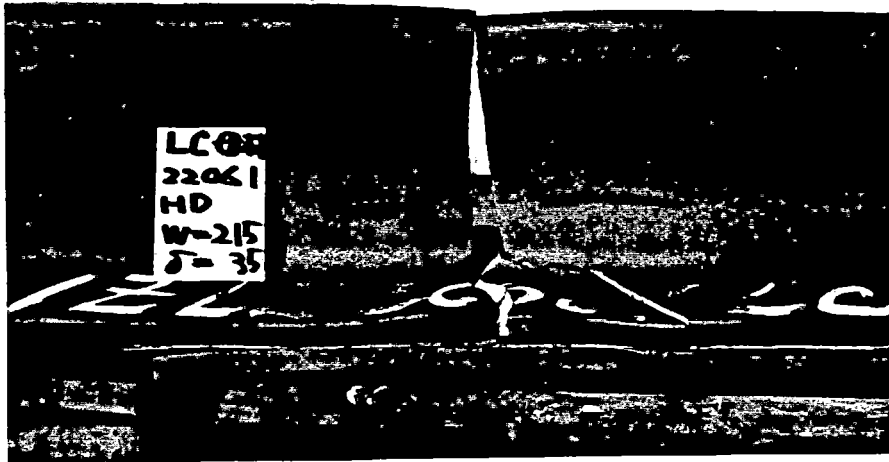RUBBING MARKS ON WEB/BASE PIECE

CHEVRONS

Figure B-6 Reconstruction of Subject Rail

(a) Rail 22063, tested in head-up position simulating
vertical wheel load on rail head

(b) Rail 22061, tested in head-down position inducing
reverse bending (tension in rail head)

FIGURE B-7. RESULTS OF JNR SLOW-BEND TEST

Information was also obtained from Wheeling-Pittsburgh Steel, a U.S. rail supplier, on effects of torch cutting in plain carbon steel rail. Lengths of rail treated with a wear-retardant coating on the running surface were to be subjected to static three-point bending tests to determine whether the coating would spall off. The rails were torch-cut to lengths suitable for the test fixture. In some cases, the rails themselves unexpectedly started to fail during the bend test, the failure mode consisting of web cracks propagating from the torch-cut ends.

Additional metallurgical tests of the subject rail were performed in the UP laboratories. Three tensile specimens were tested with the following results:

Test No.	YS(ksi)	UTS(ksi)	Elongation (%)	RA(%)
1	105.2	172.6	8.9	9.4
2	114.5	173.3	8.6	7.6
3	122.0	177.0	9.7	8.4

The results for elongation and reduction of area suggest low ductility and, therefore, low fracture toughness. The UP also ran several charpy impact tests on specimens oriented vertically with a horizontally oriented 0.079-inch depth V-notch. In all cases the fracture surfaces were judged to be fully brittle, and the fracture energies varied only slightly with test temperature.

Temperature (°F)	70	150	250	350
Fracture energy (Ft-lb)	1.5	3	5	5

Charpy fracture energy is an approximate comparative indicator of fracture toughness for similar metals, e.g., the subject rail and other steels with simlar carbon content. Figure B-8, comparing the UP data with independent results for plain carbon rail steel, suggests that the subject rail has less fracture toughness than plain carbon rail. An empirical formula for conversion of fracture energy to fracture toughness (Besuner, 1976) has been applied to the charpy data, with the result that the fracture toughness of the subject rail is estimated to be about 44 percent of the fracture toughness for plain carbon steel at 70°F.
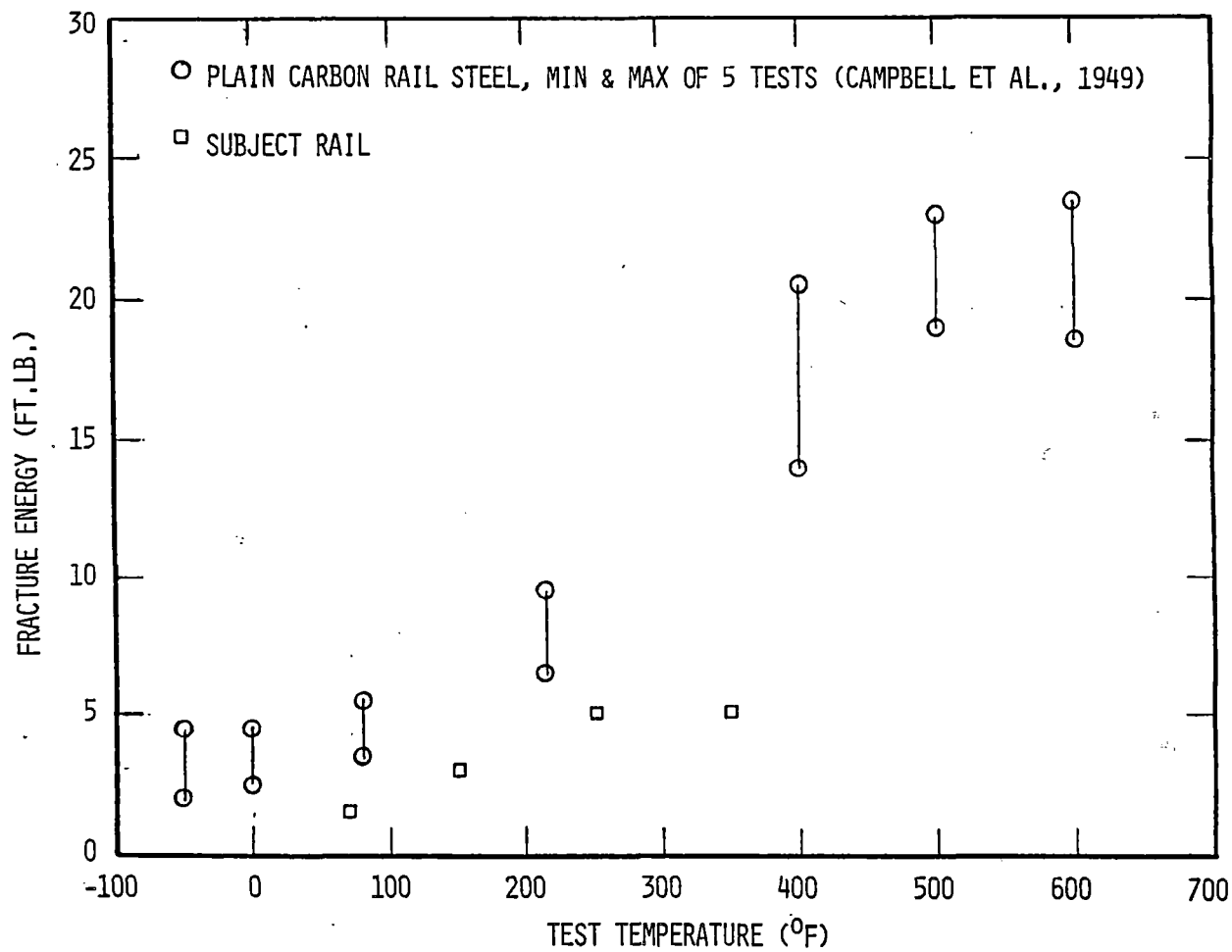
FIGURE B-8 COMPARISON OF CHARPY V-NOTCH TEST RESULTS

APPENDIX C

ASSESSMENT OF SHOCK LOADS AND STRESSES

APPENDIX C

ASSESSMENT OF SHOCK LOADS AND STRESSES

Load Sources at the Joint Crossing

1. **Vertical** - The largest load is produced as a result of a wheel moving at a constant speed along the track encountering the mismatch as a step change in height. A bound on the maximum force can be based on an assumption that the receiving rail acts as a pivot point for rolling of the wheel as shown in Figure C-1. This kinematic situation implies an impulsive vertical component of velocity, v, for the wheel,

$$v = \sqrt{\frac{2\delta}{R}} \quad V \qquad \text{(C-1.1)}$$

where:

R = wheel radius
δ = height mismatch
V = vehicle velocity

The rail forces produced as a result of this impulse can be considered as follows:

a. Unsprung Mass/Track stiffness: Assuming that the vertical impulse is a consequence of the flexibility of the rail support, as shown in Figure C-2, the dynamic force can be estimated on the basis of an analysis of the motion of the vehicle unsprung mass as it moves over a step change in vertical contact position.

From Figure C-2, the displacement of the unsprung mass M_u can be related to the movement of the rail by,

$$Z_1 = Z_0 + \delta + R \cos \theta$$

The corresponding velocity and acceleration of M_u are:

$$\frac{dZ_1}{dt} = \dot{Z}_1 = \dot{Z}_0 - R \, \dot{\theta} \, \mathrm{Sin} \, \theta \qquad \text{(C-1.2)}$$

$$\frac{d^2Z_1}{dt^2} = \ddot{Z}_1 = \ddot{Z}_0 - R \, \dot{\theta}^2 \cos \theta \approx \ddot{Z}_0 - V^2/R \qquad \text{(C-1.3)}$$

The equation of motion for the unsprung mass can be written as

$$M_u \ddot{Z}_1 + M_r \ddot{Z}_0 + K_r Z_0 = 0 \qquad \text{(C-1.4)}$$

C-3

Z_1, can be eliminated by substituting from (C-1.3) to form,

$$(M_u + M_r) \ddot{Z}_o + K_r Z_o = M_u V^2/R \qquad (C-1.5)$$

Since the rail mass is small compared with the unsprung mass, so that $M_u \gg M_r$, the solution for the motion of the rail is,

$$Z_o(t) = \frac{V^2}{R\omega_2^2} (1 - \cos \omega_2 t) + \frac{\dot{Z}_o(0)}{\omega_2} \sin \omega_2 t \qquad (C-1.6)$$

where,

$$\omega_2 = \sqrt{\frac{K_r}{M_u}} \qquad \text{and} \qquad \dot{Z}_o(0) = - V \sqrt{\frac{2\delta}{R}}$$

so that,

$$Z_o(t) = \frac{V^2}{R\omega_2^2} (1 - \cos \omega_2 t) - \frac{V}{\omega_2} \sqrt{\frac{2\delta}{R}} \sin \omega_2 t$$

The rail force resulting from this response is given by:

$$F_2(t) = - K_r Z_o(t) = \frac{-M_u V^2}{R} (1 - \cos \omega_2 t) +$$

$$V \sqrt{K_r M_u} \sqrt{\frac{2\delta}{R}} \sin \omega_2 t \qquad (C-1.6)$$

Defining $d = \frac{\sqrt{2R\delta}}{V}$

$$F_2(t) = \sqrt{K_r M_u} \; V \sqrt{\frac{2\delta}{R}} \left[\sin \omega_2 t - \frac{1}{\omega_2 d} (1 - \cos \omega_2 t) \right] \qquad (C-1.7)$$

This force reaches a maximum when,

$$\frac{dF_2}{dt} = 0$$

i.e. $\qquad \tan \omega_2 t_m = \omega_2 d$

so that the maximum rail force is given by

$$P_2 = P_o + \sqrt{K_r M_u} \; V \sqrt{\frac{2\delta}{R}} \left[\sin \omega_2 t_m - \frac{1}{\omega_2 d} (1 - \cos \omega_2 t_m) \right]$$

$$\qquad (C-1.8)$$

where P_O is the static wheel load. The parameters for this estimate can be taken as follows:

For 136 lb. rail on good support, the vertical modulus = $4(10)^3$ psi, so that

the rail stiffness, $K_r = 3.3(10)^5$ lb/in

The unsprung mass on half an axle plus a wheel = 2000/386
= 5.18 lb-sec^2/in

For 33 inch wheels, $\delta/R = 0.011$ (passenger vehicle)

For 40 inch wheels, $\delta/R = 0.009$ (locomotive)

With these values $\omega_2 = 252$ rad/sec = 40 Hz

V (in/sec)	d (1/sec)	$\omega_2 d$	$\omega_2 t_m$	t_m(sec)	Sin $\omega_2 t_m$	1-cos $\omega_2 t_m$	P_2 (kips) Passenger	P_2 (kips) Locomotive
176	0.014	3.528	1.295	0.0051	0.962	0.727	25.5	23.2
880	0.0028	0.706	0.614	0.0024	0.576	0.183	53.6	48.7
1056	0.0024	0.605	0.544	0.0020	0.518	0.144	56.5	51.3
1232	0.0020	0.504	0.467	0.0018	0.450	0.107	57.0	51.8

Assuming values of:
P_O for a locomotive = 33 kips
P_O for a passenger car = 20 kips

TABLE C-1. RAIL REACTION LOAD (kips)

	10 mph	50 mph	60 mph	70 mph
Locomotive	56.2	81.7	84.3	84.8
Passenger Vehicle	45.5	73.6	76.6	77.0

This reactive load is characterized by a relatively low frequency (40 Hz) and peaks in 2 to 5 milliseconds after impact.

This load produces longitudinal bending and transverse shear stresses in the rail. The bending sresses are dominant in the rail head. In the web there are small vertical normal stresses near the head as a consequence of the web acting as an elastic foundation supporting the head. The largest stress in the web from this load is transverse shear. These stresses are distributed as shown in Figure C-3, roughly uniformly through the web, with a value given by:

$$\tau_v = \frac{P_2}{A_w} \tag{C-1.9}$$

C-5

TABLE C-2. WEB SHEAR STRESS (ksi)

	10 mph	50 mph	60 mph	70 mph
Locomotive	18.6	28.0	29.0	29.8
Passenger Vehicle	15.9	25.8	26.8	27.0

b. Rail Mass/Contact stiffness: The estimate of rail force is consistent with dynamic vertical predictions for the most common joint irregularity, a dipped joint. It has been observed that for shock loads from such low joints a localized pulse near the rail end can be related to the contact stiffness of the wheel/rail contact region. This load has been described as P_1 to distinguish it from the vertical load estimate which may be characterized as P_2.

The maximum value of this impulsive force can be estimated by modifying the analyses above to account for the contact stiffness between the wheel and rail and for the inertia of the rail.

Referring again to Figure C-2, the relationship between motion of the unsprung mass and that of the rail can be adjusted to consider the contact deformation, Δ_c

$$Z_1 = Z_o + \delta + \Delta_c + R \cos \theta \tag{C-1.10}$$

Since $K_c \gg K_r$, motion is governed by equations that relate the rail and unsprung mass displacements to the contact displacements Δ_c,

$$M_u \ddot{Z}_1 + K_c \Delta_c = 0$$

$$M_r \ddot{Z}_o - K_c \Delta_c = 0 \tag{C-1.11}$$

These equations can be combined to form,

$$M_e (\ddot{Z}_1 - \ddot{Z}_o) + K_c \Delta_c = 0 \tag{C-1.12}$$

where

$$\frac{1}{M_e} = \frac{1}{M_u} + \frac{1}{M_r} = \frac{M_u + M_r}{M_u M_r}$$

From (C-1.10), the difference in accelerations is,

$$\ddot{Z}_1 - \ddot{Z}_o = \ddot{\Delta}_c - R\dot{\theta}^2 \cos \theta \approx \ddot{\Delta}_c - \frac{V^2}{R}$$

so that,

$$M_e \ddot{\Delta}_c + K_c \Delta_c = M_c \frac{V^2}{R} \tag{C-1.13}$$

The solution of this equation for the time variation of contact displacement is,

$$\Delta_c = \frac{V^2}{R\omega_1^2} (1 - \cos \omega_1 t) + \frac{\dot{\Delta}_c(0)}{\omega_1} \sin \omega_1 t \tag{C-1.14}$$

with,

$$\omega_1 = \sqrt{\frac{K_c}{M_e}}$$

or,

$$\Delta_c = \frac{V^2}{R\omega_1^2} (1 - \cos \omega_1 t) - \frac{V}{\omega_1} \sqrt{\frac{2\delta}{R}} \sin \omega_1 t$$

Again using

$$d = \sqrt{\frac{2R\delta}{V}}$$

$$P_1(t) = - K_c \Delta_c = \sqrt{K_c M_e} \; V \sqrt{\frac{2\delta}{R}} \; [\sin \omega_1 t - \frac{1}{\omega_1 d} (1 - \cos \omega_1 t)]$$

The maximum of this force occurs for

$$\tan \omega_1 t_m = \omega_1 d$$

Taking into account the curvature of the receiving edge of the rail at the step irregularity, we can estimate the maximum P_1 force assuming,

$$K_c = 5 (10)^6 \text{ lb/in}$$

$$M_r = 0.324 \text{ lb-sec}^2/\text{in}$$

so that

$$M_e = 0.305 \text{ lb} - \sec^2/\text{in}$$

and

$$\omega_1 = 4049 \text{ rad/sec} = 645 \text{ Hz}$$

With these values,

$$\omega_1 d \gg 1 \text{ for all speeds of interest and } \quad t_m \approx \frac{\pi}{2\omega_1}$$

Therefore, the maximum impulsive force can be approximated by:

$$P_1 = P_o + \sqrt{K_c M_e} \quad V \quad \sqrt{2\delta/R} \tag{C-1.15}$$

Table C-3 tabulates these impulsive loads for both the locomotive and the passenger vehicles.

TABLE C-3. IMPULISVE LOAD (kips)

	10 mph	50 mph	60 mph	70 mph
Locomotive	62.5	179	208	237
Passenger Vehicle	52.5	181	213	245

· This load has a high characteristic frequency, 645 Hz, and peaks in about 0.4 milliseconds.

While the vertical components of load at the mismatched joint have the largest magnitude, significant axial and lateral loads may also occur.

2. **Axial (longitudinal) forces at the mismatch** - As a wheel hits a vertical mismatch in height, an axial change in momentum occurs along with the vertical impulse. Considering the kinematic assumptions of Figure C-1, the change in axial velocity during impact is

$$V - V' = V - V \cos \theta = V - V (1 - \delta/R) = V \, \delta/R$$

Assuming that the impulsive force is provided by the axial flexibility of the rail, the maximum axial force can be estimated by:

$$P_a = (\delta/R) \, V \sqrt{K_a M_u} \tag{C-2.1}$$

Using a representative value of $5(10)^4$ lb/in. for axial stiffness K_a, for a passenger vehicle,

$$P_a = 4.42V \tag{C-2.2}$$

C-8

while for a locomotive,

$$P_a = 3.65 \text{ V} \qquad\qquad\qquad (\text{C-2.3})$$

in which the unit of V is in./sec.
Table C-4 tabulates these forces for both vehicles.

TABLE C-4. AXIAL LOAD (lbs)

	10 mph	50 mph	60 mph	72 mph
Locomotive	644	3210	3850	4620
Passenger Vehicle	780	3890	4667	5600

These loads are small in comparison with the vertical loads at the mismatch. This load does not have a significant effect unless the vertical step becomes very large. Furthermore, the resulting longitudinal stresses have little influence on the propagation of a horizontally oriented crack.

3. **Lateral forces at the mismatch** - The magnitude of lateral load is strongly determined by the specific dynamic conditions (e.g. angle of attack) that characterize the approach to the joint. Since these details cannot be known, the only available simple bound is to assume that L/W = 1 if no wheel climb has occurred. (W = Vertical wheel load)

While the reference W could be taken as large as P_2, a more reasonable estimate can be based on the static wheel load adjusted for speed. For example, the AREA speed factor for vertical load estimates the dynamic wheel load as:

$$W = P_0 \left[1 + \frac{33V}{100D} \right] \qquad\qquad (\text{C-3.1})$$

where:

V = speed (mph)

D = wheel diameter (in.)

P_0 = static wheel load (lb.)

Using this vertical load as an upper bound for the lateral load, the estimate of lateral loads is shown in table C-5.

TABLE C-5. LATERAL LOAD (kips)

	10 mph	50 mph	60 mph	70 mph
Locomotive	36.3	46.6	49.3	52.1
Passenger Vehicle	22.0	30.0	32.0	34.0

It is likely that the actual lateral load was much lower than this estimate. However, this load is potentially the most damaging to the top of the web since it can produce a vertical tensile stress at the surface. A decisive question in this regard is whether a horizontal web crack loaded in this way can be propagated horizontally.

4. **Joint bar load transfer** - As a wheel crosses from one rail to another of a bolted joint, bending of the rail places the joint bar in four point bending. This situation yields a lower stiffness than an identical length of continuous rail and produces a quasi-static upward load on the under side of the rail head. The magnitude of this upward load depends on the wheel load, and the integrity of the joint. Under some circumstances it can exceed the wheel load in magnitude. However, the major influence of this load is on alternating stresses in the vicinity of the first bolt hole rather than in the region at the end of the rail.

5. **Wheel "hop"** - A related effect of the impact of a wheel on the step irregularity in rail heights is the likelihood of temporary loss of contact of the wheel and rail. Some sources have suggested that loss of contact will occur at any step except at very low speed. A crude estimate of the height of such motion can be based on the kinematics used in Figure C-1. Equating the kinetic energy of the unsprung mass with the vertical velocity of the initial impact to some of the work needed to lift the wheel load to a height h, and the energy to deflect the primary spring by h yields,

$$h \approx \left(\frac{P_o}{M_u \omega_o^2} \right) \left[\sqrt{1 + \frac{V^2}{\left(\frac{P_o}{M_u \omega_o} \right)^2}} - 1 \right] \qquad (C-5.1)$$
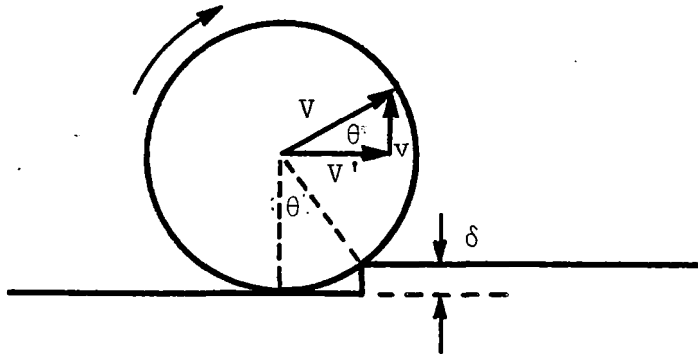
where

$\omega_o =$ Frequency of the unsprung mass on the primary vehicle suspension

For a passenger vehicle, this estimate bounds the movement of the wheel.
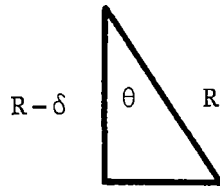
TABLE C-6. MAXIMUM HEIGHT

	10 mph	60 mph	72 mph
h	0.005 in	1.10 in	1.42 in

C-10

$$v = V \sin\theta$$

$$V' = V \cos\theta$$

$$\cos\theta = \frac{R-\delta}{R} = \left(1 - \frac{\delta}{R}\right)$$

$$\sin\theta = \sqrt{1 - \left(1 - \frac{\delta}{R}\right)^2} \approx \sqrt{2\frac{\delta}{R}} \quad \text{for small } \frac{\delta}{R}$$

$$v = \sqrt{2\frac{\delta}{R}}\ V \qquad\qquad V' = \left(1 - \frac{\delta}{R}\right) V$$

FIGURE C-3
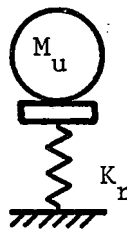
FIGURE C-2

VERTICAL SHEAR STRESS

τ_{xz}

τ_{xy}

τ_{xy}
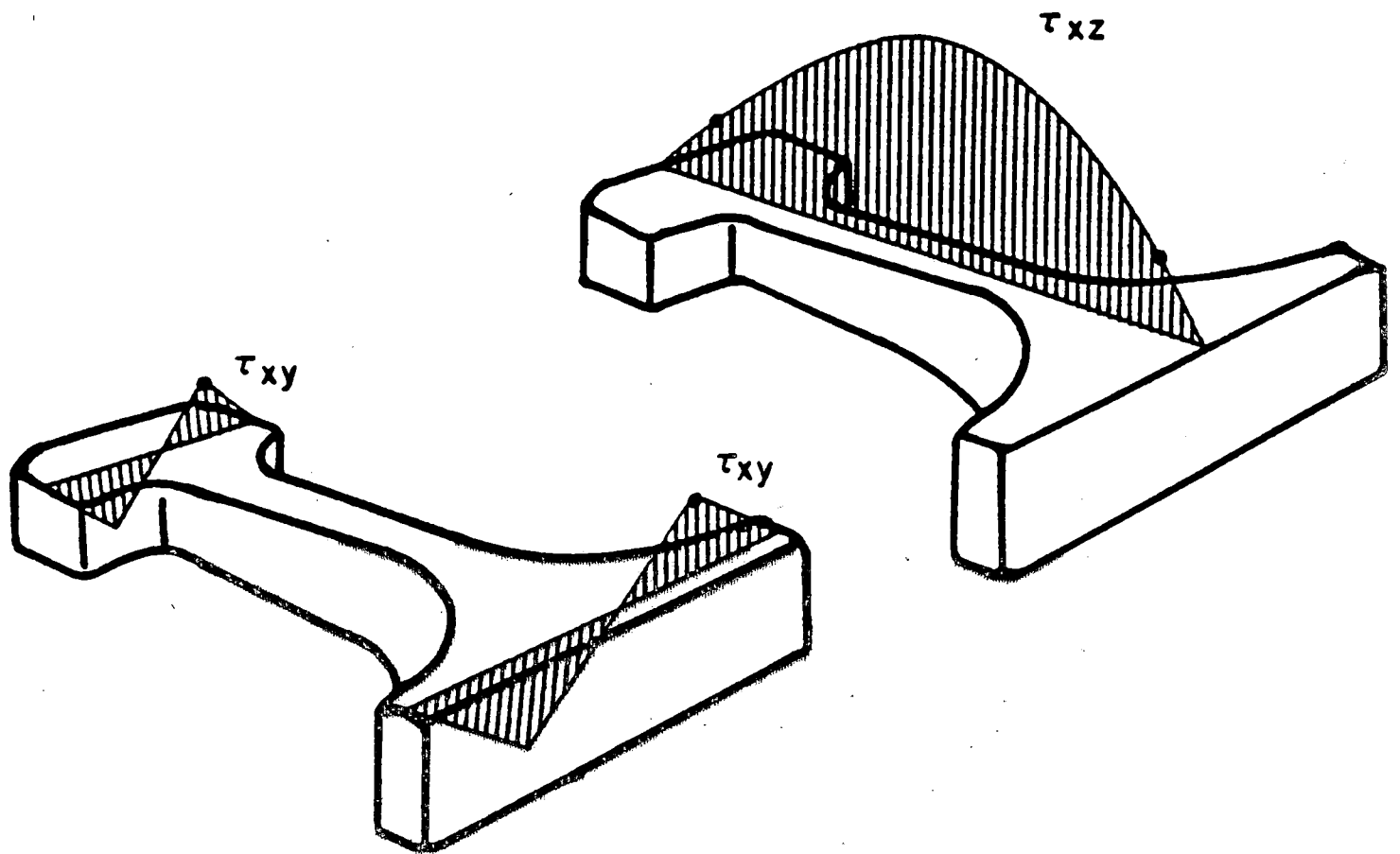
Figure C-3

RAILROAD ACCIDENT INVESTIGATION

ACCIDENT REPORT 8-83

MISSOURI PACIFIC RAILROAD COMPANY

NATIONAL RAILROAD PASSENGER CORPORATION

WOODLAWN, TEXAS

NOVEMBER 12, 1983

FEDERAL RAILROAD ADMINISTRATION

OFFICE OF SAFETY

WASHINGTON, D. C. 20590

Synopsis

On November 12, 1983, at approximately 10:10 a.m., 4 passengers
died and 133 other passengers and 12 railroad employees were
injured as the result of the derailment of an Amtrak passenger
train operating on Missouri Pacific (MP) track near Woodlawn, TX.

Location and Method of Operations

The passenger train was derailed at milepost 55.6, 3.1 miles east
of Woodlawn, on a single main track whose traffic is governed by
signal indications from a traffic control system. Woodlawn, 58.7
miles west of Texarkana, AK, is on that portion of the MP
extending from Texarkana to Dallas, TX.

Track and Terrain

In the immediate accident area, the track extends north to south
geographically. Timetable direction (the reference used) is east
to west.

From the east, there are in succession: tangent of 1 1/2 miles;
a curve of 1 degree 24 minutes to the south for 1,358.5 feet to
the point of the derailment and 433.2 feet beyond; a tangent of
157.4 feet; and a curve of 1 degree 2 minutes to the north. The

grade for the 1,600 feet approaching the derailment is 0.03 percent descending to the west, and the terrain is wooded and slightly rolling.

The main track was composed of 136-lb, RE-section continuous welded rail (CWR), laid in 1983, on crossties spaced an average of 19 1/2 inches center-to-center, and double-shoulder tie plates, spiked with two plate-holding spikes and two rail-holding spikes per plate. The rail was restrained from longitudinal displacement by an average of 48 rail anchors for every 39 feet of track, with every second tie box anchored. The ballast was crushed rock, an average of 12 inches deep below the crossties.

Sight Distance

Vision from a train approaching the accident point was restricted to approximately 900 feet by the growth of vegetation and a 1-degree 24-minute curve to the left.

Maximum Authorized Speed

The maximum authorized speed at the accident site is 75 mph for passenger trains and 60 mph for freight trains.

Applicable Rules

Federal Track Safety Standards (Code of Federal Regulations, Title 49, Part 213

Subsection 213.121(e): In the case of continuous welded rail track, each rail must be bolted with at least two bolts at each joint.

(Missouri Pacific Railroad Company Rules)

Chief Engineer's Instructions CE237T

Rails may be cut with a saw, nicked with a chisel and broken, or cut with a torch. Rails cut with a torch must be re-cut with a saw. Except in emergencies or under special conditions, all rails will be cut with a saw. Those rails cut with a torch will have a 10 mph slow order until the rails are replaced. Under no circumstances will the bolt holes be installed with a torch. All bolt holes will be drilled.

Operating Rules

Rules 350. Stop indication per Rule 292:
. . . when a train or engine is stopped by a

Stop indication and such indication does not
change promptly to a more favorable
indication:

1. Communicate with train dispatcher or
    control operator if means of communica-
    tion is available.

2. Upon verbal advice from train dispatcher
    or control operator in words: "There is
    no opposing train in the block", train
    or engine may proceed at Low Speed to
    the next signal.

Definitions:

Low Speed. A speed that will permit
stopping short of train, engine,
obstruction, or switch not properly
lined and looking out for broken rail,
but not exceeding 20 miles per hour.

Circumstances Prior to the Accident

On October 20, 1983, MP track crews replaced rail through the
accident site with new 136-lb, RE-section CWR. The rail was
chrome-vanadium alloy steel rolled by Krupp in the Federal
Republic of Germany.

On November 12, the day of the accident, MP Extra 3228 West,
consisting of two locomotives, 62 freight cars, and a caboose,
departed Texarkana at 3:32 a.m. It was stopped at 6:13 a.m. by a
signal indication displaying a "STOP" aspect at the west end of
the siding at Jefferson, TX. The dispatcher authorized Extra
3228 West to proceed in accordance with Rule 350, and the train
operated at "Low Speed" without incident from Jefferson to
Woodlawn. After the passage of Extra 3228 West, the dispatcher's
traffic control panel continued to show a track occupancy light
in the segment between Jefferson and Woodlawn.

An MP track inspector was sent by the train dispatcher to look
for a broken rail as a possible cause of the track occupancy
indication between Jefferson and Woodlawn. The inspector found a
broken field weld with the rail ends separated 3 1/2 inches at
milepost 55.6, and he removed the track from service at 6:49 a.m.

An MP track maintenance crew, composed of a foreman, a welder,
and a laborer, was sent to repair the rail. They cut the 136-lb
rail in track with an oxy-acetylene torch, 19 feet 3 inches west
of the broken weld and removed the 19-foot 3-inch section of rail.
Then they cut a section of rail (136 lb 19 feet 6 inches) from
the secondhand rail that had been removed from the track on
October 20. This section of rail was cut with the torch at both
ends. Thirty-six-inch joint bars were used to join the

3

replacement rail to the rail on the track. At 9:15 a.m., the MP
track inspector restored the track to service with no
restrictions.

MP Extra 3319 West, two locomotives, 97 freight cars, and a
caboose, departed Texarkana at 3:50 a.m., stopped at Jefferson at
6:46 a.m., and waited for the track beyond Jefferson to be
restored to service. At 9:30 a.m., the dispatcher authorized
Extra 3319 West to proceed with no speed restrictions. The track
crew remained on the scene and actually observed the train move
over the repaired track at milepost 55.6 at the maximum
authorized speed (60 mph) without incident.

Passenger Extra Amtrak 294 West, consisting of two locomotives
and nine passenger cars, departed Texarkana at 9:07 a.m. This
train, designated Number 21, "The Eagle," was an extra train
placed in service to facilitate a timetable change on November 13.
Aboard were 145 passengers, 12 Amtrak passenger service
employees, and 5 MP train service employees. When 294 West
passed Jefferson at 10:03 a.m., the signal at the west end of
Jefferson displayed an aspect indicating "Proceed," and the
intermediate signal at milepost 53.1 also showed "Proceed." The
fireman was operating the locomotive, and the engineer was seated
in the fireman's seat.

The Accident

At about 10:10 a.m., as Passenger Extra Amtrak 294 West was
traveling at about 72 mph over the repaired track at milepost
55.6, the eight rear cars became derailed. The CWR adjoining the
western end of the replacement rail shattered into small pieces
under the train during the derailing action. When the leading
locomotive stopped 1,274 feet west of the point of derailment,
the two locomotives and the first car remained on the track, and
the next four derailed cars remained essentially upright. The
sixth car was derailed and was leaning approximately 40 degrees
to the north. The seventh, eighth, and ninth cars were derailed
and rested on their north sides, after they had slid on their
sides along the ground north of the track. (See figure 1.)

Emergency Response

At 10:10 a.m., the crew of Passenger Extra Amtrak 294 West
radioed news of the accident to the train dispatcher. The
Marshall Fire Department, the Texas Department of Public Safety,
and the Harrison County Sheriff's Department were notified by
10:20 a.m. The Harrison County sheriff immediately requested
areawide assistance, and 23 organizations responded.

The first ambulance arrived at 10:30 a.m., and by 11:15 a.m. all
the seriously injured were evacuated. Two physicians and one
nurse from Marshall Memorial Hospital reached the scene at 10:40
a.m., and evacuation of all casualties was completed by 11:30 a.m.
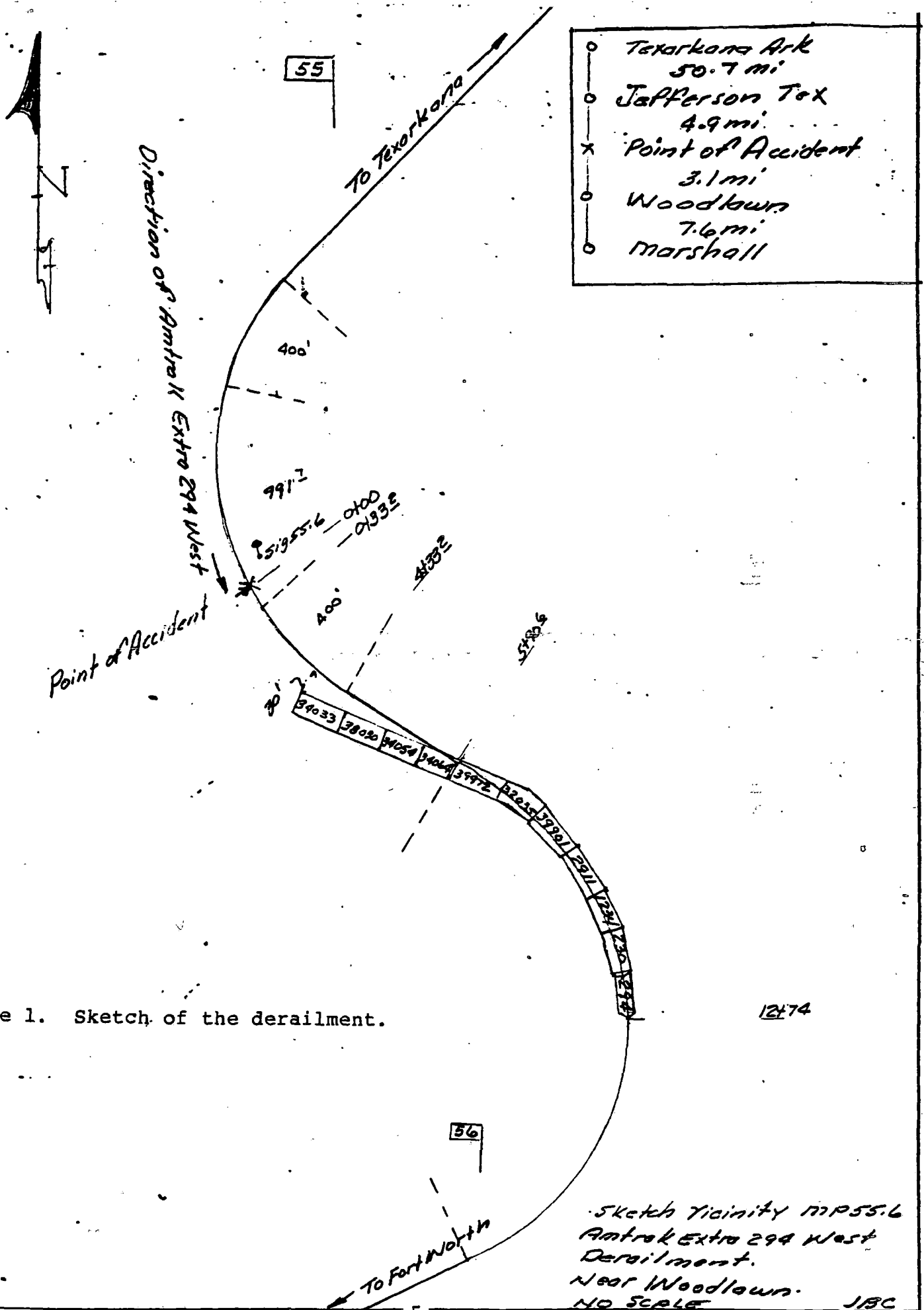The medical staff of Marshall Memorial Hospital was increased

4

Figure 1. Sketch of the derailment.

from 6 to 15 physicians before the first casualties arrived at
11:20 a.m. Casualties were also transported to hospitals in
Jefferson and Longview, TX. Uninjured passengers were taken to
the Texas Army National Guard Armory at Marshall.

Damage

Four passenger cars received substantial damage; four passenger
cars sustained minor damage. The carriers (MP and Amtrak)
estimated damage to equipment at $2,111,500 and damage to track
at $11,000.

Post-accident Examination of Equipment

On November 13, 1983, tests of the air brakes on the entire
consist of Passenger Extra Amtrak 294 West showed that the brakes
functioned properly on the two locomotive units and the first
four cars of the train. The brakes on the rear five cars were
inoperative because of derailment damage. The right
leading-wheel flange of the second car (sleeping car No. 2911)
showed the mark of a heavy impact.

Post-accident Examination of Track Structure

Examination of the track revealed that the north rail, starting
at the west joint of the replaced rail section and continuing
west for 38 feet, had shattered into many small pieces, 85 of
which were later recovered. The first mark of a derailment was
found on the south rail, 7 feet 11 inches west of the west joint
of the replacement rail. The only deviations from Federal Track
Safety Standards were the two joints securing the replacement
rail--each had only three bolts instead of the required four.
Otherwise, the condition of the track had met the requirements of
Federal Track Safety standards.

Analyses of recovered pieces of the failed rail and the adjacent
sections of rail revealed the following:

o   The failed rail branding was marked ."136 RE VT KRUPP
     1981 111111111 AL."

o   The failed rail shattered into more than 85 pieces
     within 38 feet. (Some pieces were not recovered.)
     Generally, the failure followed a longitudinal crack in
     the web of the rail, with secondary cracks progressing
     through the head and base of the rail.

o   The eastern end of the failed rail had been cut with a
     torch. A step or offset of approximately one-eight
     inch in the cut was found approximately 2 inches below
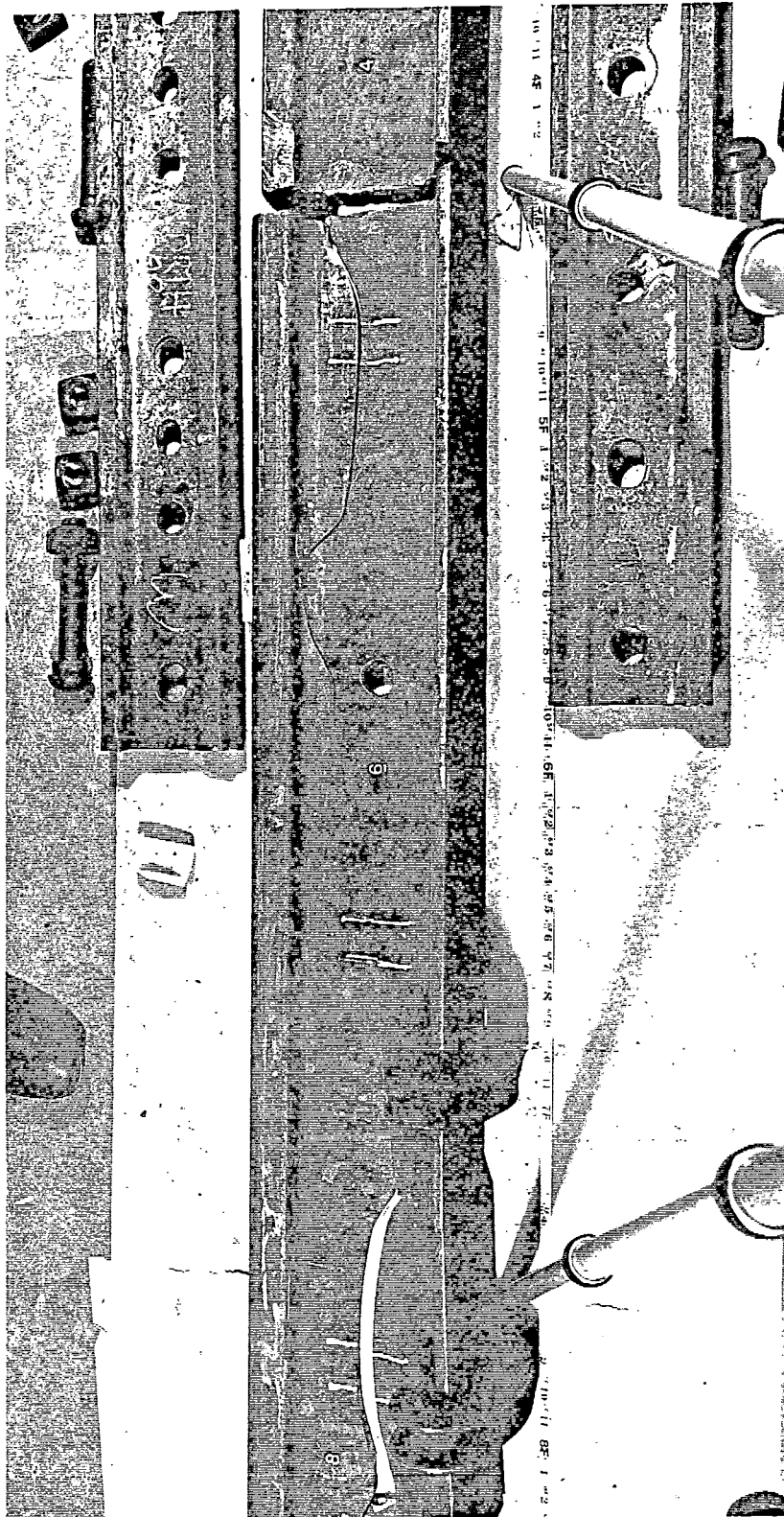   the tread surface of the rail. (See figure 2.)

6

Figure 2.

East end of failed chrome-vanadium rail, adjoining west end
of replacement rail sections at the right. Reconstructed,
with joint bars removed.

o   The eastern end of the longitudinal crack in the failed
    rail was located at the offset in the torch cut. (See
    figure 3.)

o   When the joint connecting the failed rail with the
    replacement section was reconstructed, there was a
    tread mismatch of approximately three-sixteenths inch,
    with the failed rail tread higher than the replacement
    rail. (See figure 4.)

o   The eastern and western ends of the replacement rail
    section each contained two bolt holes, drilled a
    diameter of 1 1/8 inches. The two ends of the CWR
    which were connected to the replacement rail section
    each contained only one bolt hole, drilled a diameter
    of 1 1/8 inches.

o   MP track inspection records showed that the track had
    been inspected at the frequency required by the Federal
    Track Safety Standards.

o   A rail flaw detector car had last been operated over
    the main track at the accident site on June 1,
    1983--before the failed rail was installed. The only
    rail defect found within 1 mile of the accident site
    was a small, defective plant weld in the north rail at
    milepost 55.2.

o   One week after the accident, a rail flaw detector car
    was used to test all the high-alloy rail on the Dallas
    Subdivision, including the recently installed Krupp
    chrome-vanadium rail; no flaws were detected.

Findings

1. At the time of the accident, Passenger Extra Amtrak 294
    West was being operated in accordance with the
    carrier's (MP) applicable rules and regulations.

2   The MP failed to issue the proper speed restrictions
    when it restored service over torch-cut rails without
    reducing train speed to 10 mph -- a violation of the
    Missouri Pacific Chief Engineer's Instruction CE237T.

3. The track at the accident site -- in non-compliance
    with 49 CFR 213.121 (e) -- had two bolt holes drilled
    the required diameter in both ends of the replacement
    rail, but only one bolt hole was drilled the required
    diameter in the CWR rail ends. Three bolts were
    provided at each connecting joint in violation of the
    four-bolt hole requirement.

8

Figure 3.

East face of failed chrome-vanadium rail, reconstructed, showing torch cut, offset, and web crack through offset.
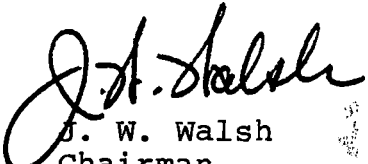
Figure 4.

Failed rail on the left, reconstructed, joined to west end of replacement rail section, showing bolting pattern and tread surface mismatch.

Note: Mismatch is slightly exaggerated due to separation of top and bottom portions of failed rail of the web crack.

4. As a result of the unusual failure, FRA established a technical Task Force to conduct a full evaluation of the rail failure. The Task Force concluded that "there are no inherent reasons why acceptable combinations of manufacturing, operating, and maintenance practices cannot result in safe use of alloy rail." Further, the Task Force recommended, "torch-cutting of rails should not be preferred practice for temporary track repairs. However, railroads which do so to alloy rail should restrict the speed allowed over those repairs to 10 mph."

5. The traffic control signal system functioned as intended--first detecting the broken field weld and later displaying the "Proceed" signal after the continuity of the track circuit had been restored by repair of the rail.

Dated at Washington, D.C.,
this 25 day of July
by the Federal Railroad Administration

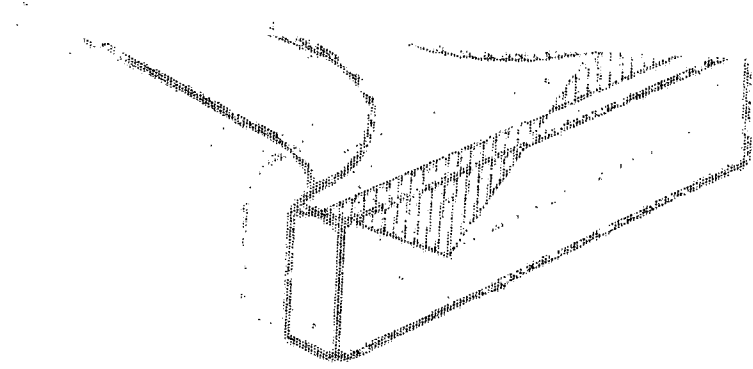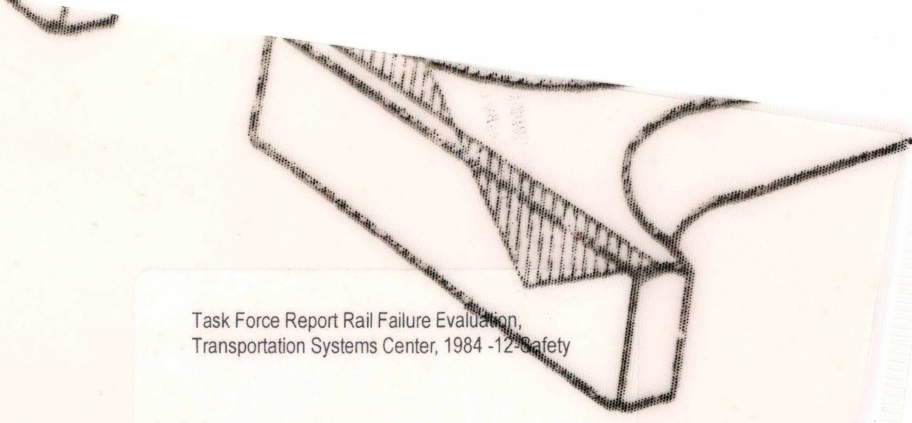J. W. Walsh
Chairman
Railroad Safety Board

11

Figure C-9

Task Force Report Rail Failure Evaluation,
Transportation Systems Center, 1984 -12-Safety